



Photo by David Oliete - www.davidoliete.com

3DGenomics

Methods, challenges and who knows what...

Marc A. Marti-Renom

<http://marciuslab.org>
<http://3DGenomes.org>
<http://cnag.crg.eu>

cnag **CRG**  **ICREA**

Human Genome / Genome Interactions



Capturing Chromosome Conformation

Job Dekker,^{1*} Karsten Rippe,² Martijn Dekker,³ Nancy Kleckner⁴

We describe an approach to detect the frequency of interaction between any two genomic loci. Generation of a matrix of interaction frequencies between sites on the same or different chromosomes reveals their relative spatial disposition and provides information about the physical properties of the chromatin fiber. This methodology can be applied to the spatial organization of entire genomes in organisms from bacteria to human. Using the yeast *Saccharomyces cerevisiae*, we could confirm known qualitative features of chromosome organization within the nucleus and dynamic changes in that organization during meiosis. We also analyzed yeast chromosome III at the G₁ stage of the cell cycle. We found that chromatin is highly flexible throughout. Furthermore, functionally distinct AT- and GC-rich domains were found to exhibit different conformations, and a population-average 3D model of chromosome III could be determined. Chromosome III emerges as a contorted ring.

Important chromosomal activities have been linked with both structural properties and spatial conformations of chromosomes. Local properties of the chromatin fiber influence gene expression, origin firing, and DNA repair [e.g., (1, 2)]. Higher order structural features—such as formation of the 30-nm fiber, chromatin loops and axes, and inter-chromosomal connections—are important for chromosome morphogenesis and also have roles in gene expression and recombination. Activities such as transcription and timing of replication have been related to overall spatial nuclear disposition of different regions and their relationships to the nuclear envelope [e.g., (3–6)]. At each of these levels, chromosome organization is highly dynamic, varying both during the cell cycle and among different cell types.

Analysis of chromosome conformation is complicated by technical limitations. Electron microscopy, while affording high resolution, is laborious and not easily applicable to studies of specific loci. Light microscopy

affords a resolution of 100 to 200 nm at best, which is insufficient to define chromosome conformation. DNA binding proteins fused to green fluorescent protein permit visualization of individual loci, but only a few positions can be examined simultaneously. Multiple loci can be visualized with fluorescence in situ hybridization (FISH), but this requires severe treatment that may affect chromosome organization.

We developed a high-throughput methodology, Chromosome Conformation Capture (3C), which can be used to analyze the overall spatial organization of chromosomes and to investigate their physical properties at high resolution. The principle of our approach is outlined in Fig. 1A (7). Intact nuclei are isolated (8) and subjected to formaldehyde fixation, which cross-links proteins to other proteins and to DNA. The overall result is cross-linking of physically touching segments throughout the genome via contacts between their DNA-bound proteins. The relative frequencies with which different sites have become cross-linked are then determined. Analysis of genome-wide interaction frequencies provides information about general nuclear organization as well as physical properties and conformations of chromosomes. We have used intact yeast nuclei for all experiments. Although the method can be performed using intact cells, the signals are considerably lower, making quantification difficult (9). The general nuclear organization

of purified nuclei is largely intact, as shown below.

For quantification of cross-linking frequencies, cross-linked DNA is digested with a restriction enzyme and then subjected to ligation at very low DNA concentration. Under such conditions, ligation of cross-linked fragments, which is intramolecular, is strongly favored over ligation of random fragments, which is intermolecular. Cross-linking is then reversed and individual ligation products are detected and quantified by the polymerase chain reaction (PCR) using locus-specific primers. Control template is generated in which all possible ligation products are present in equal abundance (7). The cross-linking frequency (X) of two specific loci is determined by quantitative PCR reactions using control and cross-linked templates, and X is expressed as the ratio of the amount of product obtained using the cross-linked template to the amount of product obtained with the control template (Fig. 1B). X should be directly proportional to the frequency with which the two corresponding genomic sites interact (10).

Control experiments show that formation of ligation products is strictly dependent on both ligation and cross-linking (Fig. 1C). In general, X decreases with increasing separation distance in kb along chromosome III (“genomic site separation”). Cross-linking frequencies for both the left telomere and the centromere of chromosome III with each of 12 other positions along that same chromosome (Fig. 1, C and D) were determined using nuclei isolated from exponentially growing haploid cells. Interestingly, the two telomeres of chromosome III interact more frequently than predicted from their genomic site separation, which suggests that the chromosome ends are in close spatial proximity. This is expected because yeast telomeres are known to occur in clusters (11, 12).

We next applied our method to an analysis of centromeres and of homologous chromosomes (“homologs”) during meiosis in yeast. This analysis provides information about general nuclear organization as well as physical properties and conformations of chromosomes. We have used intact yeast nuclei for all experiments. Although the method can be performed using intact cells, the signals are considerably lower, making quantification difficult (9). The general nuclear organization

REPORTS

antibody to chicken Cu (H1) [Southern Biotechnology Associates, Birmingham, AL] and then with polyclonal fluorescein isothiocyanate-conjugated goat antibodies to mouse IgG (Fab), [Sigma]. Prodomerently spg(4-) subunits were excluded from the analysis, because they most likely originated from cells that were already spg(4-) at the time of subcloning.

23. For Ig light chain sequencing, PCR amplification and sequencing of the rearranged light chain V segments were performed as previously described (19), except that high-fidelity PfuTurbo polymerase (Stratagene) was used with primer pair VA1/VA2 for PCR, and primer VA3 was used for sequencing (17). Only one nucleotide change, which most likely reflects a PCR-introduced artifact, was noticed in the V_H-J_H heteroduplex region in a total of 80 0.5-kb-long sequences from AID^{-/-} cells.

24. We thank M. Roth and T. Brunner for kindly providing the McCremer plasmid vector; P. Carninci and Y. Hayashizaki for construction of the riken1 bursal cDNA library; A. Peters and K. Jablonski for excellent technical help; and C. Stoeck and J. Lubber for carefully reading the manuscript. Supported by grant No. 631/2-1 from the Deutsche Forschungsgemeinschaft, by the European Union Framework V programs “Chicken Image” and “Genetics in a Cell Line,” and by Japan Society for the Promotion of Science Postdoctoral Fellowships for Research Abroad.

22 October 2001; accepted 18 December 2001

*Broad Institute of Harvard and Massachusetts Institute of Technology (MIT), MA 02139, USA. ²Division of Health Sciences and Technology, MIT, Cambridge, MA 02139, USA. ³Program for Evolutionary Dynamics, Department of Organismic and Evolutionary Biology, Department of Mathematics, Harvard University, Cambridge, MA 02138, USA. ⁴Department of Applied Mathematics, Harvard University, Cambridge, MA 02138, USA. ⁵Program in Gene Function and Expression and Department of Biochemistry and Molecular Pharmacology, University of Massachusetts Medical School, Worcester, MA 01605, USA. ⁶Tried Hutchinson Cancer Research Center, Seattle, WA 98109, USA. ⁷Department of Radiation Oncology, University of Washington School of Medicine, Seattle, WA 98195, USA. ⁸Department of Genome Sciences, University of Washington, Seattle, WA 98195, USA. ⁹Department of Pathology, Harvard Medical School, Boston, MA 02115, USA. ¹⁰Department of Pediatrics, University of Washington, Seattle, WA 98195, USA. ¹¹Department of Physics, MIT, Cambridge, MA 02139, USA. ¹²Department of Biology, MIT, Cambridge, MA 02139, USA. ¹³Department of Systems Biology, Harvard Medical School, Boston, MA 02115, USA.

*To whom correspondence should be addressed. E-mail: dekker@mit.edu

1306 15 FEBRUARY 2002 VOL 295 SCIENCE www.sciencemag.org

Comprehensive Mapping of Long-Range Interactions Reveals Folding Principles of the Human Genome

Erez Lieberman-Aiden,^{1,2,3,4,*} Nynke L. van Berkum,^{5*} Louise Williams,¹ Maxim Imakaev,² Tobias Ragozy,^{6,7} Agnes Telling,^{6,7} Ido Amit,¹ Bryan R. Lajole,⁸ Peter J. Sabo,⁸ Michael O. Dorschner,⁸ Richard Sandstrom,⁸ Bradley Bernstein,^{8,9} M. A. Bender,¹⁰ Mark Groudine,^{1,2,11} Andreas Gnirke,¹² John Stamatoyannopoulos,¹³ Leonid A. Mirny,¹¹ Eric S. Lander,^{1,2,12,13} Job Dekker^{1*}

We created a Hi-C library from a karyotypically normal human lymphoblastoid cell line (GM06990) and sequenced it on two lanes of an Illumina Genome Analyzer (Illumina, San Diego, CA), generating 8.4 million read pairs that could be uniquely aligned to the human genome reference sequence; of these, 6.7 million corresponded to long-range contacts between segments >20 kb apart.

We constructed a genome-wide contact matrix *M* by dividing the genome into 1-Mb regions (“loci”) and defining the matrix entry *m_{ij}* to be the number of ligation products between locus *i* and locus *j* (10). This matrix reflects an ensemble average of the interactions present in the original sample of cells; it can be visually represented as a heatmap, with intensity indicating contact frequency (Fig. 1B).

We tested whether Hi-C results were reproducible by repeating the experiment with the same restriction enzyme (HindIII) and with a different one (NotI). We observed that contact matrices for these new libraries (Fig. 1, C and D) were extremely similar to the original contact matrix [Pearson’s *r* = 0.990 (HindIII) and *r* = 0.814 (NotI); *P* was negligible (<10⁻³⁰⁰) in both cases]. We therefore combined the three data sets in subsequent analyses.

We first tested whether our data are consistent with known features of genome organization (1): specifically, chromosome territories (the tendency of distant loci on the same chromosome to be near one another in space) and patterns in subnuclear positioning (the tendency of certain chromosome pairs to be near one another).

We calculated the average interchromosomal contact probability, *L_{ij}*(*s*), for pairs of loci separated by a genomic distance *s* (distance in base pairs along the nucleotide sequence) on chromosome *n*. *L_{ij}*(*s*) decreases monotonically on every chromosome, suggesting polymer-like behavior in which the 3D distance between loci increases with increasing genomic distance; these findings are in agreement with 3C and fluorescence in situ hybridization (FISH) (6, 11). Even at distances greater than 200 Mb, *L_{ij}*(*s*) is always much greater than the average contact probability between different chromosomes (Fig. 2A). This implies the existence of chromosome territories.

Interchromosomal contact probabilities between pairs of chromosomes (Fig. 2B) show that small, gene-rich chromosomes (chromosomes 16, 17, 19, 20, 21, and 22) preferentially interact with each other. This is consistent with FISH studies showing that these chromosomes frequently colocalize in the center of the nucleus

The three-dimensional (3D) conformation of chromosomes is involved in compartmentalizing the nucleus and bringing widely separated functional elements into close spatial proximity (1–5). Understanding how chromosomes fold can provide insight into the complex relationships between chromatin structure, gene activity, and the functional state of the cell. Yet beyond the scale of nucleosomes, little is known about chromatin organization.

Here, we report a method called Hi-C that adapts the above approach to enable purification of ligation products followed by massively parallel sequencing. Hi-C allows unbiased identification of chromatin interactions across an entire genome. We briefly summarize the process: cells are crosslinked with formaldehyde; DNA is digested with a restriction enzyme that leaves a 5’ overhang; the 5’ overhang is filled, including a biotinylated residue; and the resulting blunt-end fragments are ligated under dilute conditions that favor ligation events between the cross-linked DNA fragments. The resulting DNA sample contains ligation products consisting of fragments that were originally in close spatial proximity in the nucleus, marked with biotin at the junction. A Hi-C library is created by shearing the DNA and selecting the biotin-containing fragments with streptavidin beads. The library is then analyzed by using massively parallel DNA sequencing, producing a catalog of interacting fragments (Fig. 1A) (10).

Long-range interactions between specific pairs of loci can be evaluated with chromosome conformation capture (3C), using spatially constrained ligation followed by locus-specific polymerase chain reaction (PCR) (6). Adaptations of 3C have extended the process with the use of inverse PCR (4C) (7, 8) or multiplexed ligation-mediated amplification (SC) (9). Still, these techniques require choosing a set of target loci and do not allow unbiased genome-wide analysis.

*Broad Institute of Harvard and Massachusetts Institute of Technology (MIT), MA 02139, USA. ²Division of Health Sciences and Technology, MIT, Cambridge, MA 02139, USA. ³Program for Evolutionary Dynamics, Department of Organismic and Evolutionary Biology, Department of Mathematics, Harvard University, Cambridge, MA 02138, USA. ⁴Department of Applied Mathematics, Harvard University, Cambridge, MA 02138, USA. ⁵Program in Gene Function and Expression and Department of Biochemistry and Molecular Pharmacology, University of Massachusetts Medical School, Worcester, MA 01605, USA. ⁶Tried Hutchinson Cancer Research Center, Seattle, WA 98109, USA. ⁷Department of Radiation Oncology, University of Washington School of Medicine, Seattle, WA 98195, USA. ⁸Department of Genome Sciences, University of Washington, Seattle, WA 98195, USA. ⁹Department of Pathology, Harvard Medical School, Boston, MA 02115, USA. ¹⁰Department of Pediatrics, University of Washington, Seattle, WA 98195, USA. ¹¹Department of Physics, MIT, Cambridge, MA 02139, USA. ¹²Department of Biology, MIT, Cambridge, MA 02139, USA. ¹³Department of Systems Biology, Harvard Medical School, Boston, MA 02115, USA.

*These authors contributed equally to this work. To whom correspondence should be addressed. E-mail: lander@broadinstitute.org (E.S.L.); job.dekker@umassmed.edu (J.D.).

Supporting Online Material
www.sciencemag.org/cgi/content/full/1178746/DC1
Materials and Methods
SOM Text

Bill & Melinda Gates Foundation; the U.S. Agency for International Development (USAID); and the National Institute of Allergy and Infectious Diseases, NIH, R01AI05292 (D.R.B.). The contents are the responsibility of the authors and do not necessarily reflect the views of USAID or the U.S. government. The authors declare competing financial interests. Protocol G Principal Investigators: G. Miya, J. Semwaga, A. Pozniak, O. MaPhee, O. Manjari, L. Mwananyanda, E. Karita, A. Inweley, W. Jasko, J. Detschitz, L. G. Bekker, P. Pitsutthum, R. Paris, and S. Allen.

7 July 2009; accepted 28 August 2009
Published online 3 September 2009
10.1126/science.1178746
Include this information when citing this paper.

Fig. S1 to S10
Table S1 to S6
References

www.sciencemag.org SCIENCE VOL 326 9 OCTOBER 2009 289

Hi-C 3.0

Akgol Oksuz, et al. Nature Methods 2021 & keep an eye on a possible soon paper for 4DNucleome

ANALYSIS

<https://doi.org/10.1038/s41592-021-01248-7>

nature methods



OPEN

Systematic evaluation of chromosome conformation capture assays

Betul Akgol Oksuz^{1,10}, Liyan Yang^{1,10}, Sameer Abraham², Sergey V. Venev¹, Nils Krietenstein³, Krishna Mohan Parsi^{4,5}, Hakan Ozadam^{1,6}, Marlies E. Oomen¹, Ankita Nand¹, Hui Mao^{4,5}, Ryan M. J. Genga^{4,5}, Rene Maehr^{4,5}, Oliver J. Rando³, Leonid A. Mirny^{2,7,8}, Johan H. Gibcus¹✉ and Job Dekker^{1,9}✉

Chromosome conformation capture (3C) assays are used to map chromatin interactions genome-wide. Chromatin interaction maps provide insights into the spatial organization of chromosomes and the mechanisms by which they fold. Hi-C and Micro-C are widely used 3C protocols that differ in key experimental parameters including cross-linking chemistry and chromatin fragmentation strategy. To understand how the choice of experimental protocol determines the ability to detect and quantify aspects of chromosome folding we have performed a systematic evaluation of 3C experimental parameters. We identified optimal protocol variants for either loop or compartment detection, optimizing fragment size and cross-linking chemistry. We used this knowledge to develop a greatly improved Hi-C protocol (Hi-C 3.0) that can detect both loops and compartments relatively effectively. In addition to providing benchmarked protocols, this work produced ultra-deep chromatin interaction maps using Micro-C, conventional Hi-C and Hi-C 3.0 for key cell lines used by the 4D Nucleome project.

Chromosome conformation capture (3C)-based assays¹ have become widely used to generate genome-wide chromatin interaction maps². Analysis of chromatin interaction maps has led to detection of several features of the folded genome. Such features include precise looping interactions (at the 0.1–1 Mb scale) between pairs of specific sites that appear as local dots in interaction maps. Many of such dots represent loops formed by cohesin-mediated loop extrusion that is stalled at convergent CCCTC-binding factor (CTCF) sites^{3–5}. Loop extrusion also produces other features in interaction maps such as stripe-like patterns anchored at specific sites that block loop extrusion. The effective depletion of interactions across such blocking sites leads to domain boundaries (insulation). At the megabase scale, interaction maps of many organisms including mammals display checkerboard patterns that represent the spatial compartmentalization of two main types of chromatin: active and open A-type chromatin domains, and inactive and more closed B-type chromatin domains⁶.

The Hi-C protocol has evolved over the years. While initial protocols used restriction enzymes such as HindIII that produces relatively large fragments of several kilobases⁷, over the last 5 years Hi-C using DpnII or MboI digestion has become the protocol of choice for mapping chromatin interactions at kilobase resolution⁸. More recently, Micro-C, which uses MNase instead of restriction enzymes as well as a different cross-linking protocol, was shown to allow generation of nucleosome-level interaction maps^{7–9}. It is critical to ascertain how key parameters of these 3C-based methods, including cross-linking and chromatin fragmentation, quantitatively

influence the detection of chromatin interaction frequencies and the detection of different chromosome folding features that range from local looping between small intra-chromosomal (cis) elements to global compartmentalization of megabase-sized domains. Here, we systematically assessed how different cross-linking and fragmentation methods yield quantitatively different chromatin interaction maps.

Results

We explored how two key parameters of 3C-based protocols, cross-linking and chromatin fragmentation, determine the ability to quantitatively detect chromatin compartment domains and loops. We selected three cross-linkers widely used for chromatin: 1% formaldehyde (FA), conventional for most 3C-based protocols; 1% FA followed by incubation with 3 mM disuccinimidyl glutarate (the FA + DSG protocol); and 1% FA followed by incubation with 3 mM ethylene glycol bis(succinimidylsuccinate) (the FA + EGS protocol) (Fig. 1a). We selected four different nucleases for chromatin fragmentation: MNase, DdeI, DpnII and HindIII, which fragment chromatin in sizes ranging from single nucleosomes to multiple kilobases. Combined, the three cross-linking and four fragmentation strategies yield a matrix of 12 distinct protocols (Fig. 1b). To determine how performance of these protocols varies for different states of chromatin we applied this matrix of protocols to multiple cell types and cell cycle stages. We analyzed four different cell types: pluripotent H1 human embryonic stem cells (H1-hESCs), differentiated endoderm (DE) cells derived from H1-hESCs, fully

¹Program in Systems Biology, Department of Biochemistry and Molecular Pharmacology, University of Massachusetts Medical School, Worcester, MA, USA. ²Department of Physics, Massachusetts Institute of Technology, Cambridge, MA, USA. ³Department of Biochemistry and Molecular Pharmacology, University of Massachusetts Medical School, Worcester, MA, USA. ⁴Program in Molecular Medicine, University of Massachusetts Medical School, Worcester, MA, USA. ⁵Program in Molecular Medicine, Diabetes Center of Excellence, University of Massachusetts Medical School, Worcester, MA, USA. ⁶Department of Molecular Biosciences, University of Texas at Austin, Austin, TX, USA. ⁷Institute for Medical Engineering and Science, Massachusetts Institute of Technology, Cambridge, MA, USA. ⁸Graduate Program in Biophysics, Harvard University, Cambridge, MA, USA. ⁹Howard Hughes Medical Institute, Chevy Chase, MD, USA. ¹⁰These authors contributed equally: Betul Akgol Oksuz, Liyan Yang. ✉e-mail: Johan.Gibcus@umassmed.edu; Job.Dekker@umassmed.edu

NATURE METHODS

ANALYSIS

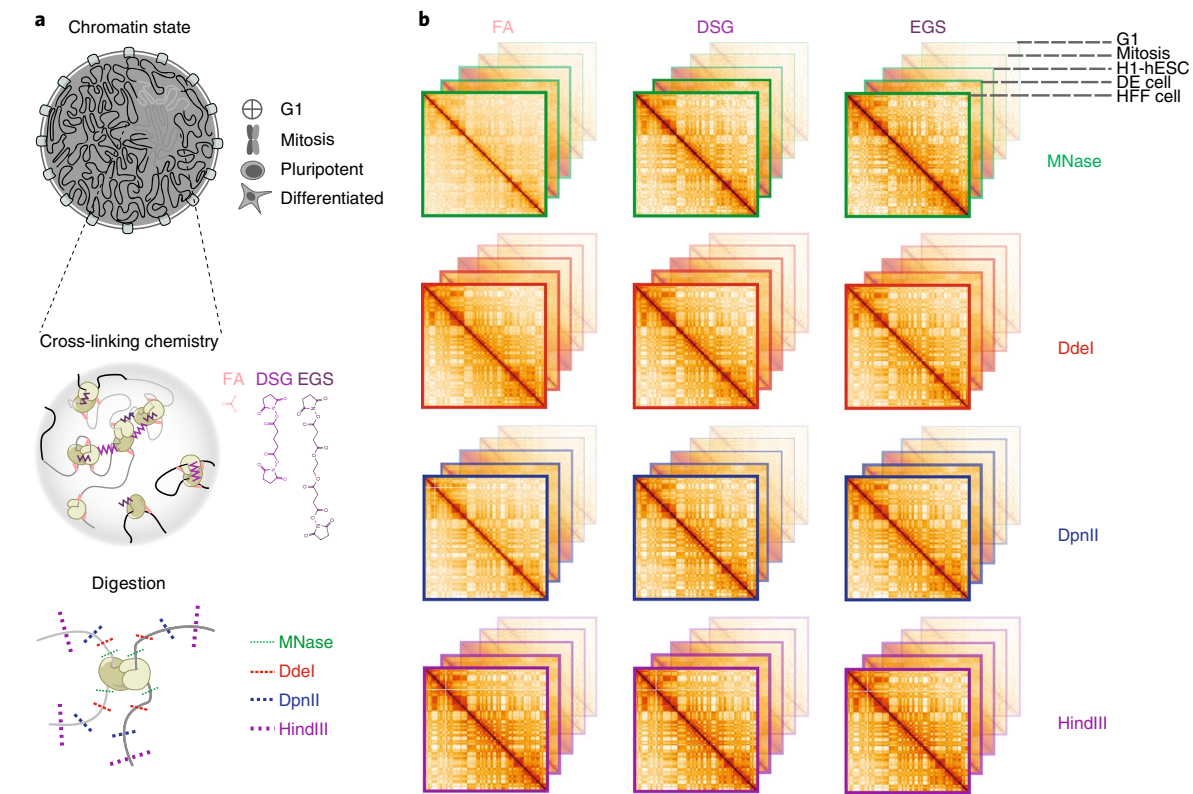


Fig. 1 | Outline of the experimental design. a, Experimental design for conformation capture for various cells, cross-linkers and enzymes. **b**, Representation of interaction maps from experiments in **a**.

differentiated human foreskin fibroblast (HFF) cells (12 protocols for each), and HeLa-S3 cells (9 protocols). We analyzed two cell cycle stages: G1 and mitosis, in HeLa-S3 cells (9 protocols for each; Fig. 1). Each interaction library was then sequenced on a single lane of a HiSeq4000 instrument, producing ~150–200 million uniquely mapping read pairs (Supplementary Table 1). We used the Distiller pipeline to align the sequencing reads, and pairtools and cooler¹⁰ packages to process mapped reads and create multi-resolution contact maps (Methods). Given that the density of restriction sites for DdeI, DpnII and HindIII fluctuates along chromosomes, we observed different read coverages in raw interaction maps obtained from datasets using these enzymes (Extended Data Fig. 1h). These differences were removed after matrix balancing¹¹.

We first assessed the size range of the chromatin fragments produced after digestion by the 12 protocols for HFF cells (Methods). Digestion with HindIII resulted in 5–20-kb DNA fragments; DpnII and DdeI produced fragments of 0.5–5 kb; and MNase protocols included a size selection step to ensure that the ligation product involved two mononucleosome-sized fragments (~150 bp) (Extended Data Fig. 1). Different cross-linkers did not affect the size ranges produced by the different nucleases, although DSG cross-linking lowered digestion efficiency slightly (Extended Data Fig. 1b).

All 3C-based protocols can differentiate between cell states. We first assessed the similarity between the 63 datasets by global and pairwise correlations using HiCRep and hierarchical clustering (Extended Data Fig. 1c)^{12,13}. We found that the datasets are highly correlated and cluster primarily by cell type and state and then by cell type similarity, for example H1-hESCs and H1-hESC-derived DE cells cluster together; and the most distinct cluster is formed by mitotic HeLa cells. MNase protocols show slightly lower correlations with Hi-C experiments.

Extra cross-linking yields more intra-chromosomal contacts. Given that chromosomes occupy individual territories, intra-chromosomal (cis) interactions are more frequent than inter-chromosomal (trans) interactions¹⁴. The cis:trans ratio is commonly used as an indicator of Hi-C library quality given that inter-chromosomal interactions are a mixture of true chromatin interactions and interactions that are the result of random ligations^{14,15}. For all enzymes and cell types, we found that the addition of DSG or EGS to FA cross-linking decreased the percentage of trans interactions (Fig. 2a for HFF and Extended Data Fig. 2a for H1-hESC, DE, HeLa-S3).

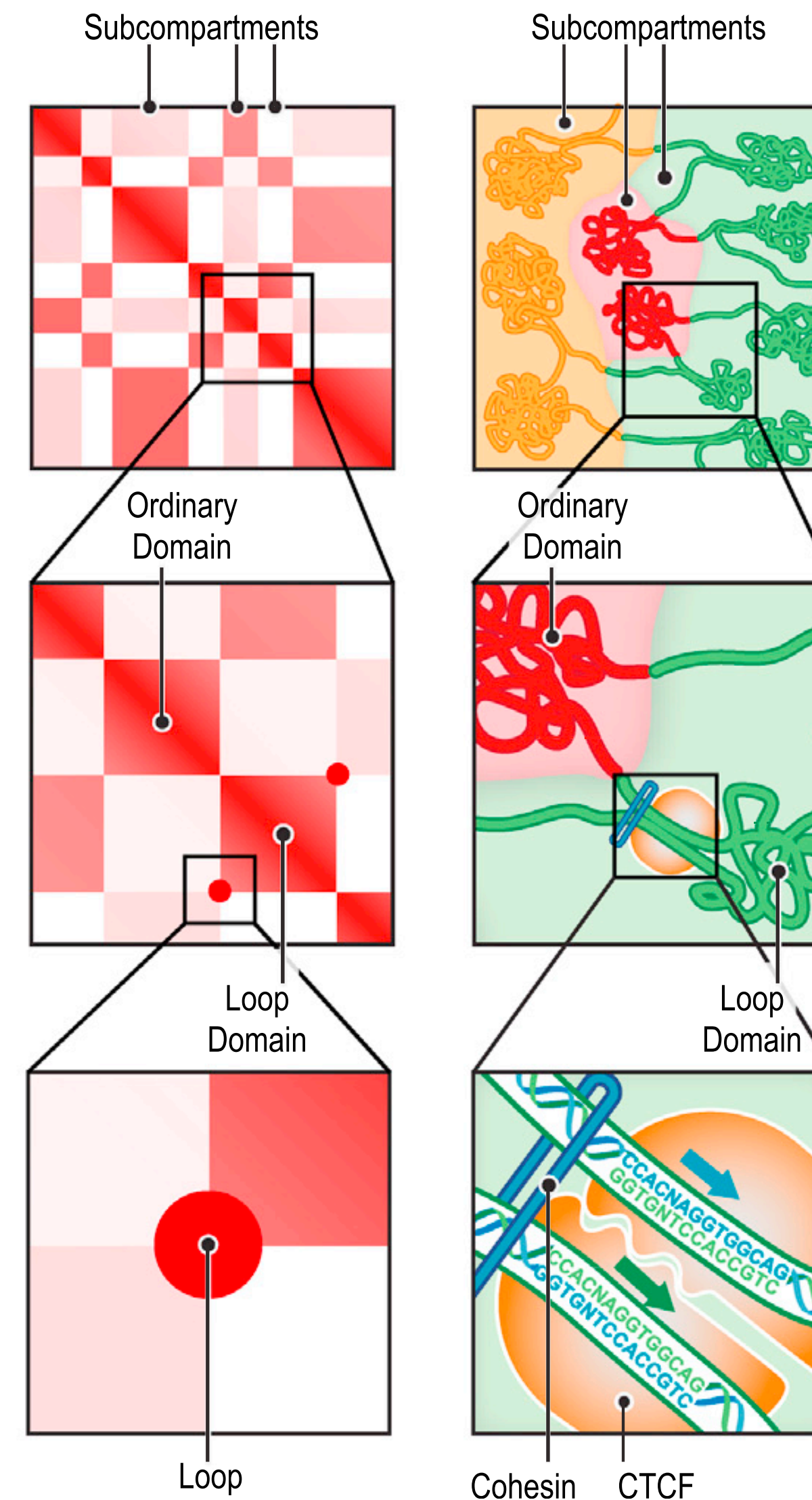
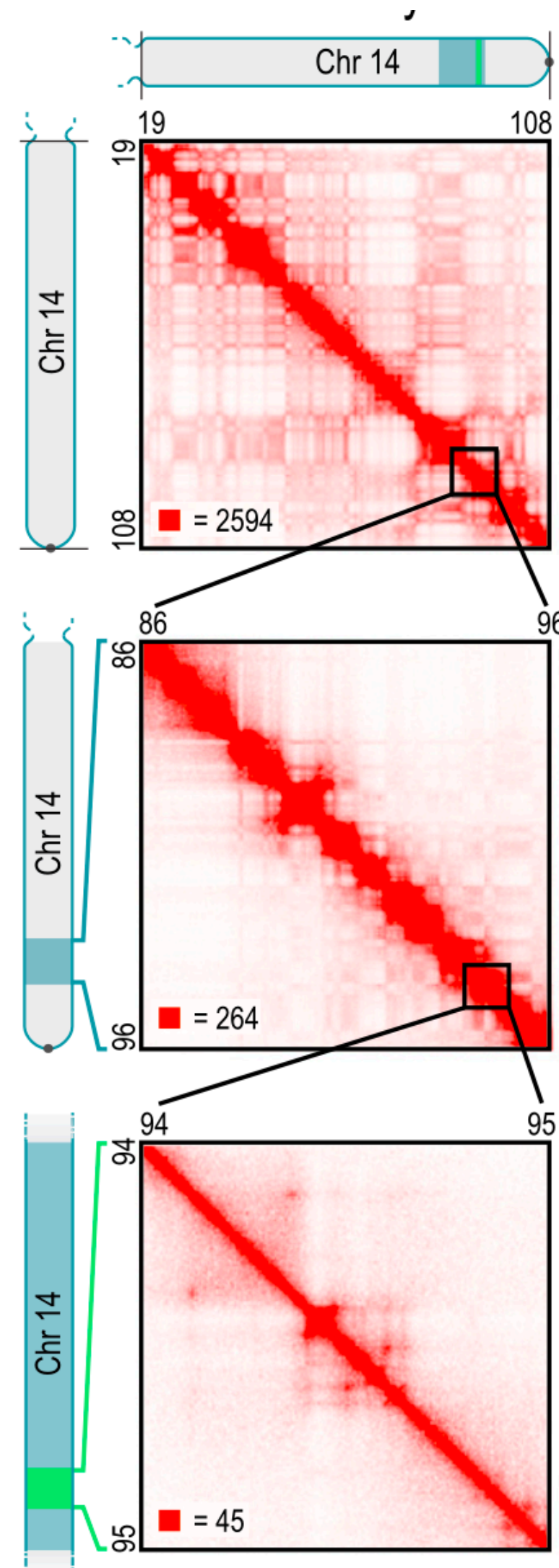
Regarding intra-chromosomal interactions, we noticed two distinct patterns. First, digestion into smaller fragments increased short-range interactions. MNase digestion generated more interactions between loci separated by less than 10 kb, whereas digestion with either DdeI, DpnII or HindIII resulted in a relatively larger number of interactions between loci separated by more than 10 kb (Fig. 2a,b for HFF and Extended Data Fig. 2a,b for DE, H1-hESC, HeLa-S3). Second, $P(s)$ plots showed that the addition of either DSG or EGS resulted in a steeper decay in interaction frequency as a function of genomic distance for all fragmentation protocols. Moreover, for a given chromatin fragmentation level, additional cross-linking with DSG or EGS reduced trans interactions, as shown for HFF cells and all other cell types and cell stages studied (Fig. 2c,d and Extended Data Fig. 2c). The addition of DSG or EGS could have reduced fragment mobility and the formation of spurious ligations, resulting in a steeper slope of the $P(s)$. We note a difference in slopes for data obtained with different cell types and cell cycle stages, which could reflect state-dependent differences in chromatin compaction.

Random ligation events between un-cross-linked, freely diffusing fragments lead to noise that is mostly seen in trans and long-range cis interactions. Experiments that use DpnII and

Hierarchical genome organisation

Lieberman-Aiden, E., et al. (2009). *Science*, 326(5950), 289–293.

Rao, S. S. P., et al. (2014). *Cell*, 1–29.



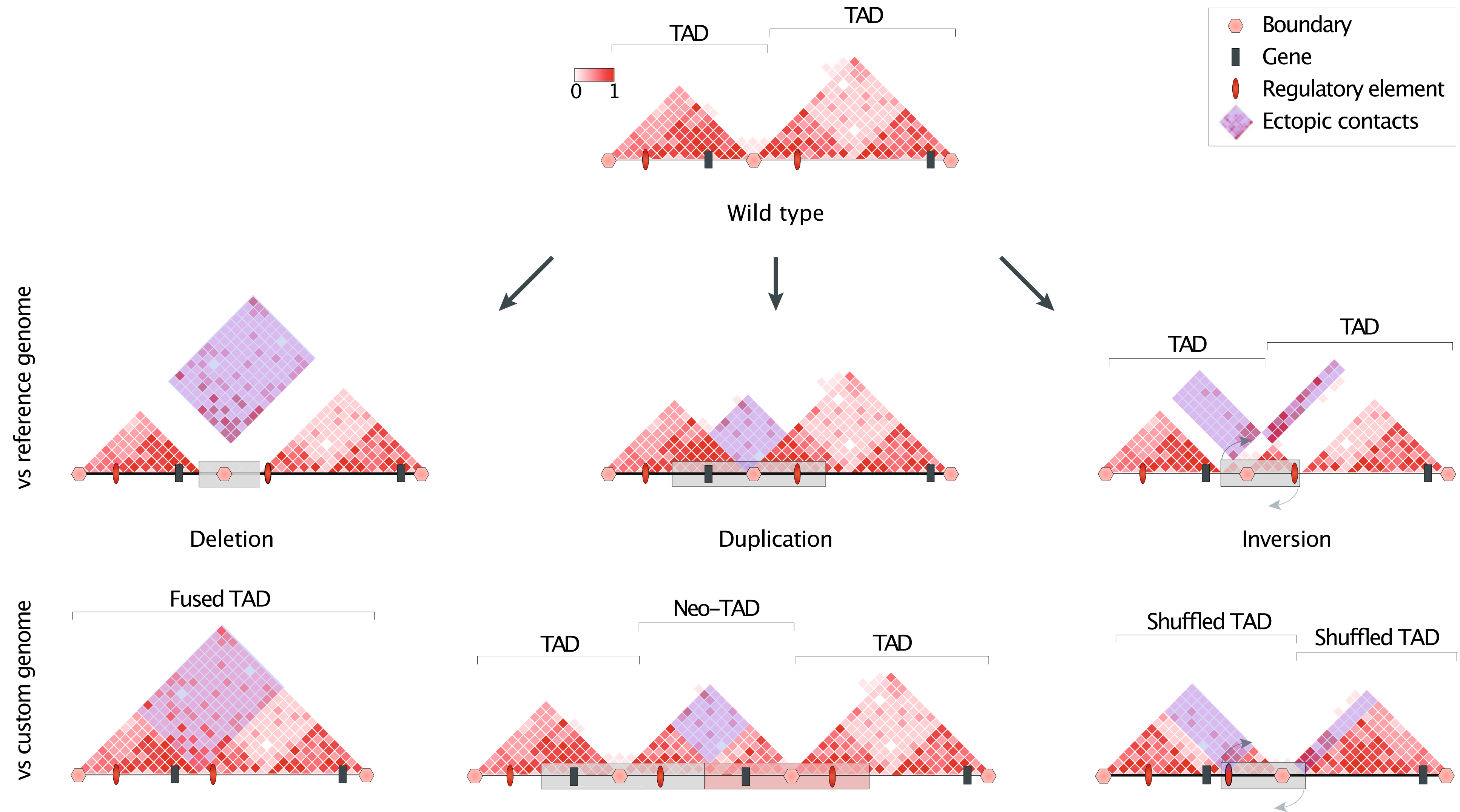
OK/Accepted

Debate!

Functional?

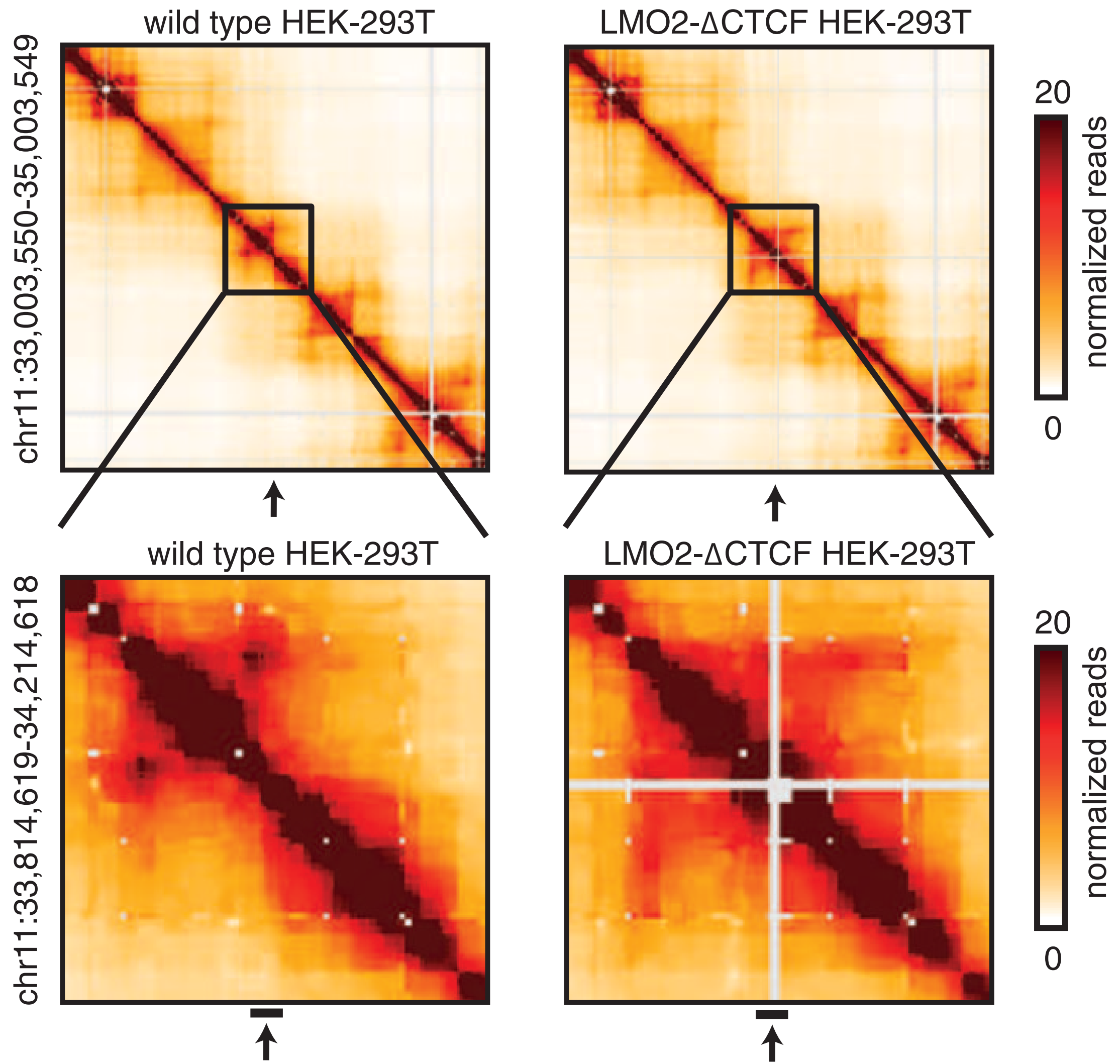
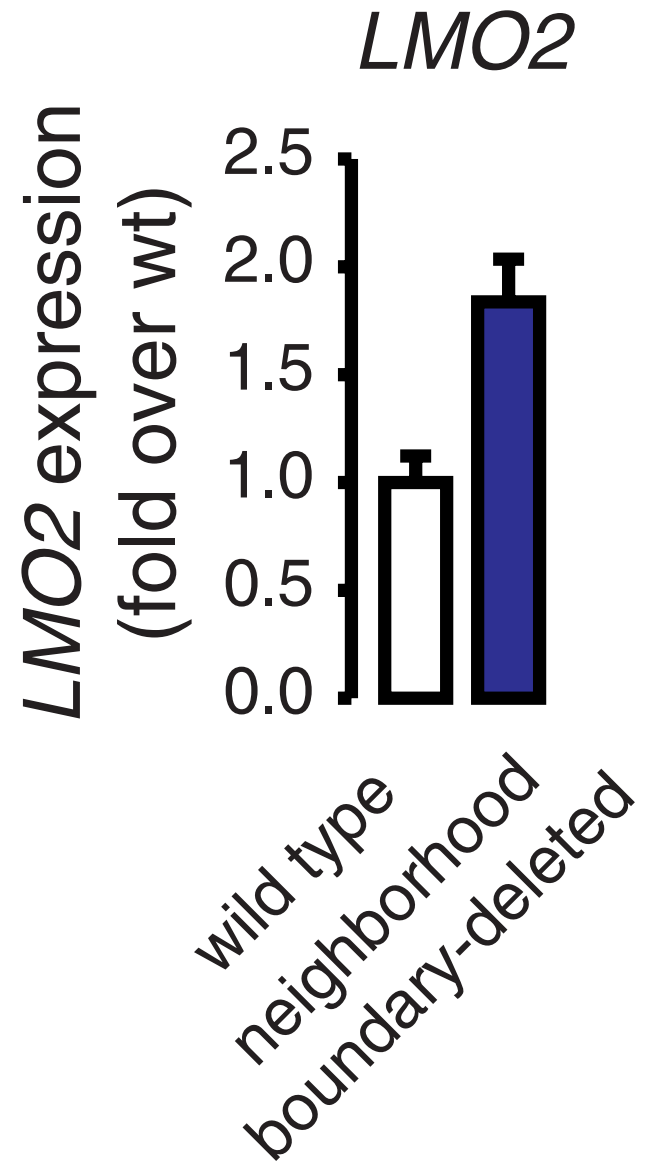
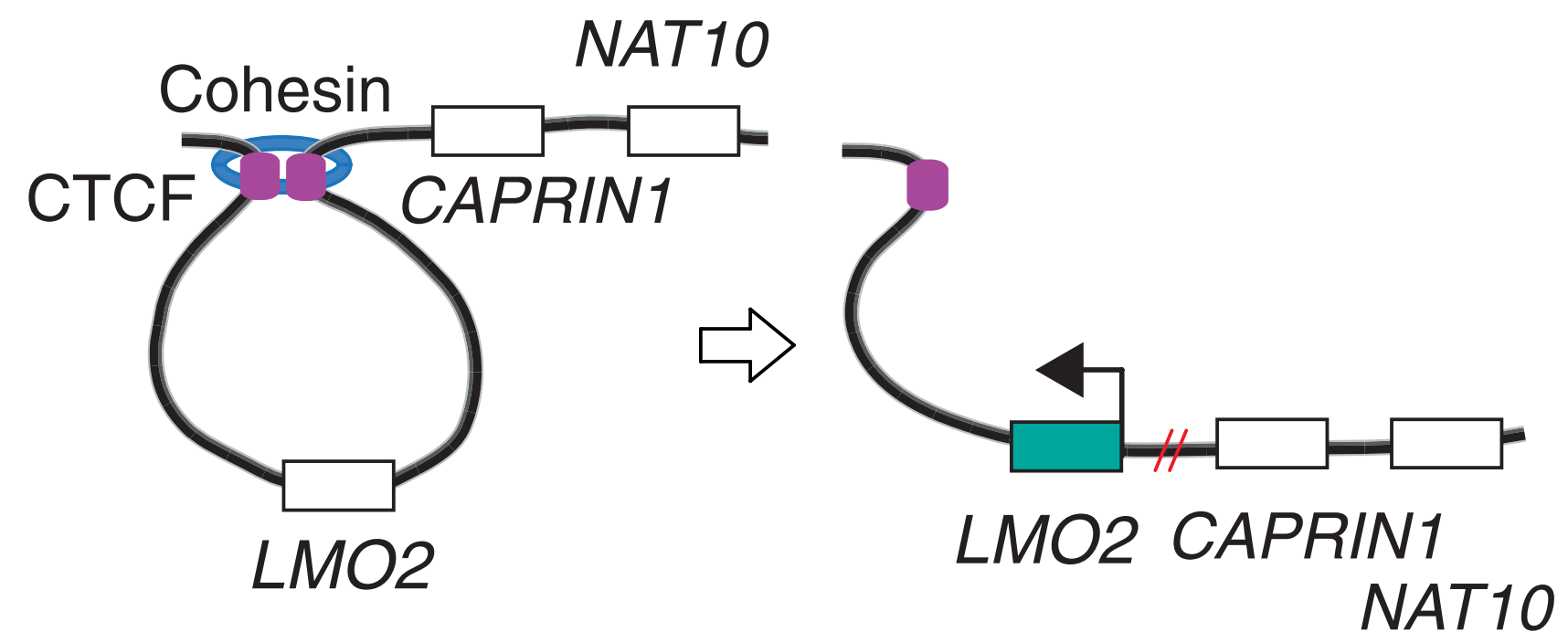
Are TADs functional units?

Spielmann Nature Reviews Genetics 2018 (19) 453–467



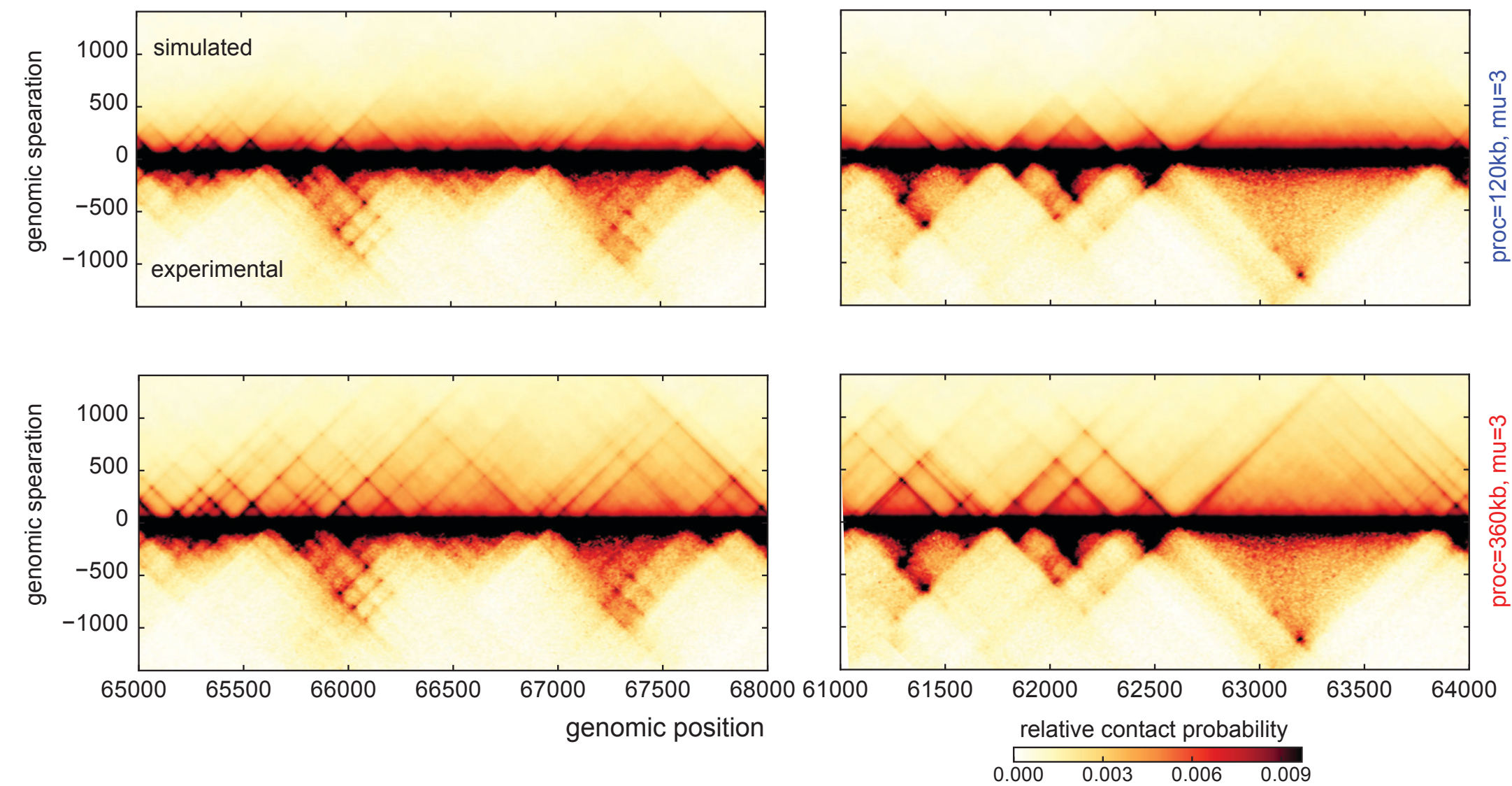
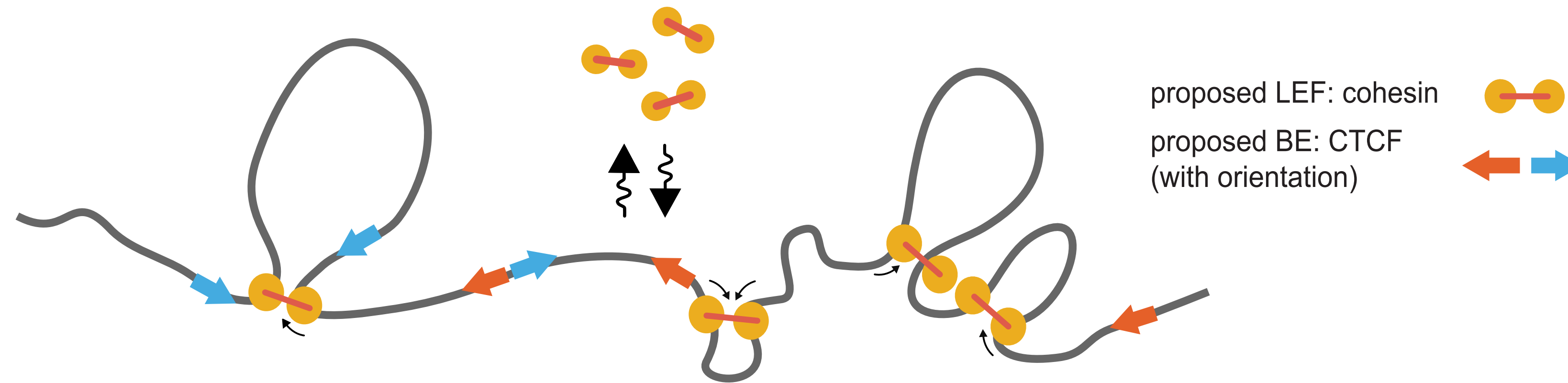
Deletion of a boundary

Hnisz, D., et al. (2016). Science



Loop-extrusion as a TAD forming mechanism

Fudenberg, G., et al. (2016) Cell Reports. & Seaborn et al. (2015) PNAS



Some questions...

Do TADs exist?

If they do, are they really "domains"?

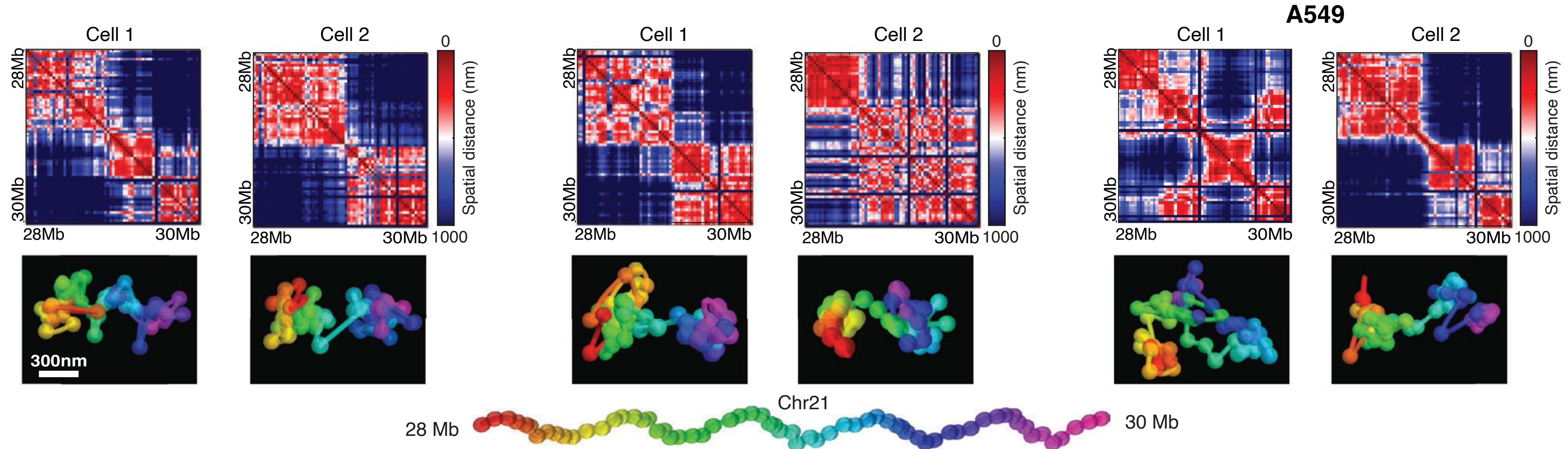
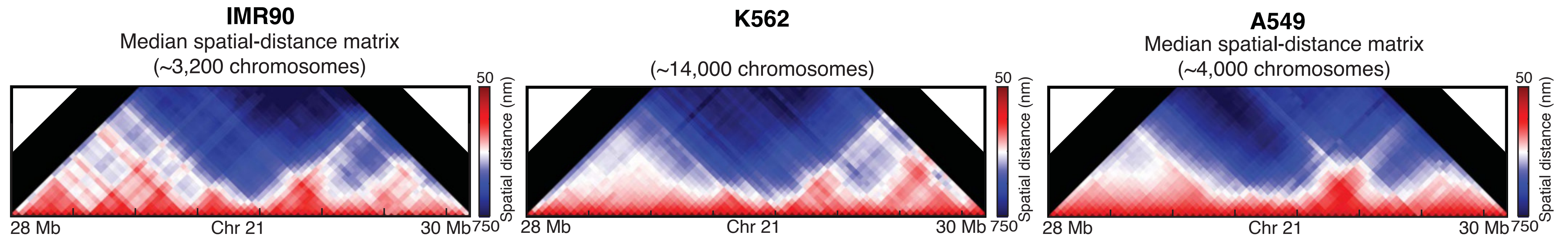
Are TADs the results of a population analysis?

Who is more important? The boundary or the TAD?

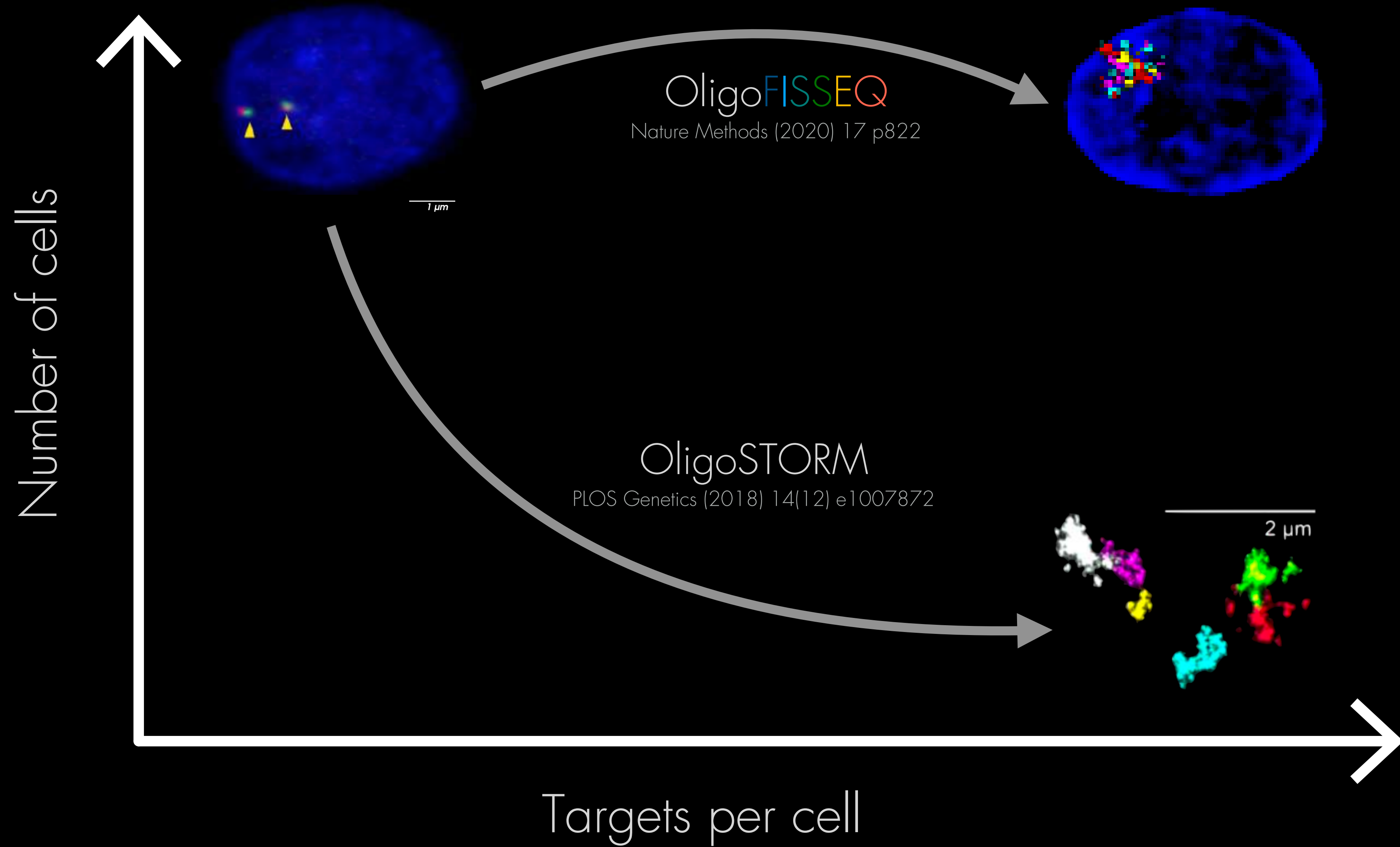
"A probabilistic (population) event that is the result of a collection of (extruded) loops whose conformational exploration depends on boundaries"

Can we see TADs?

Bintu et al. Science 2018; Mateo et al. Science 2019; Mateo et al. Nat Protocols, 2021



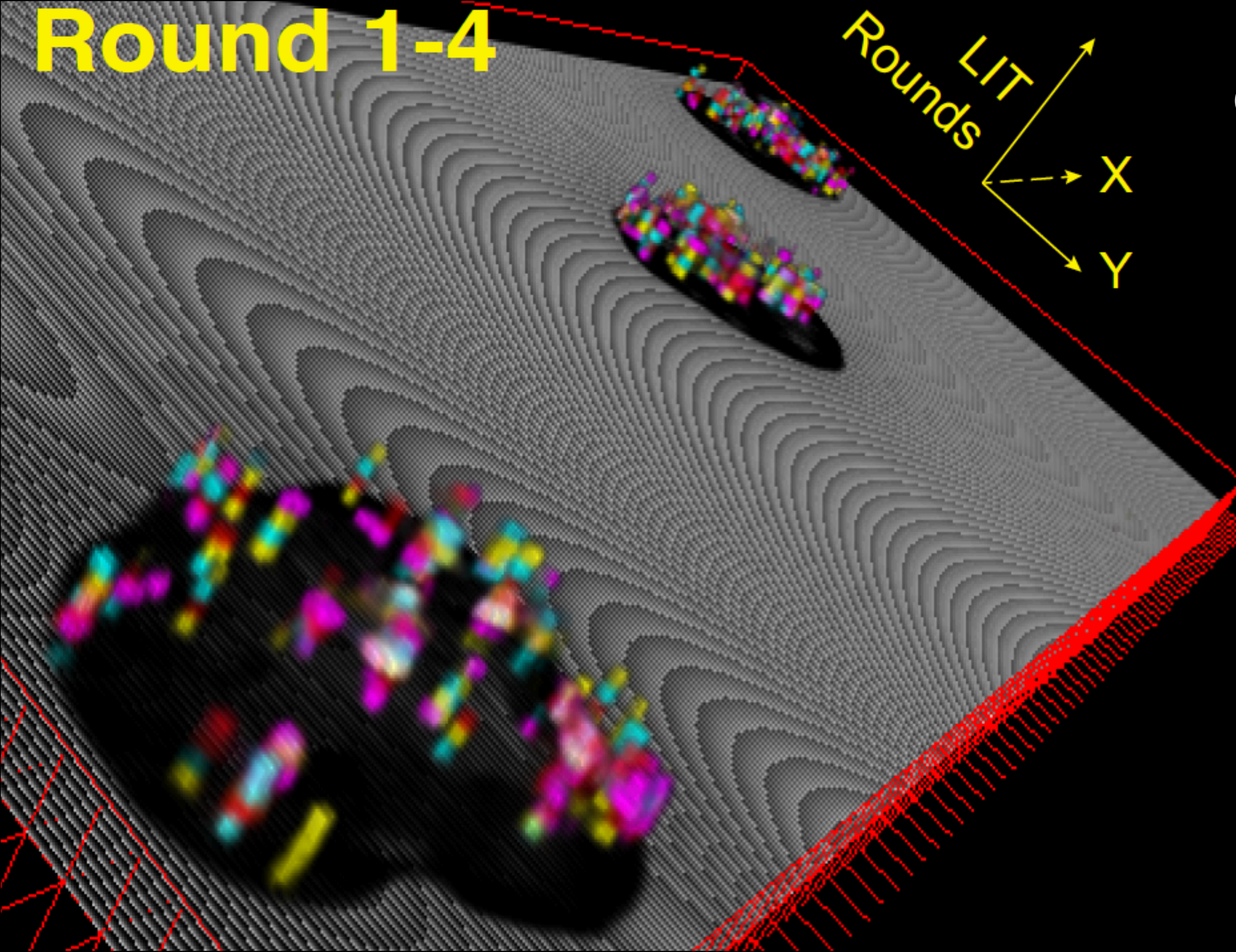
Visualizing the genome!



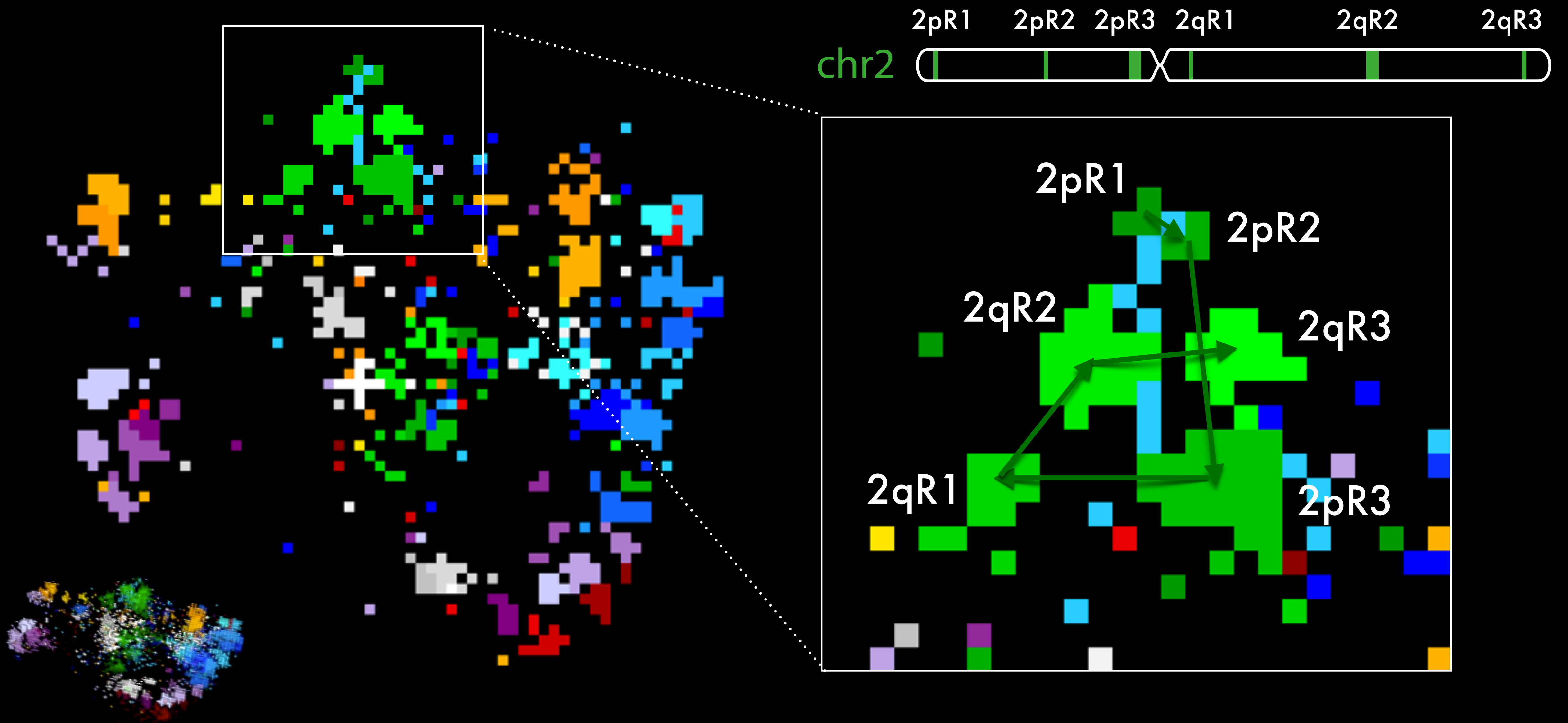
Round 1-4

LIT
Rounds
X
Y

OligoFISSEQ
"Manhattan plot"



In OligoFISSEQ every pixel matters & make "patches"



OligoFISSEQ pipelined with OligoSTORM



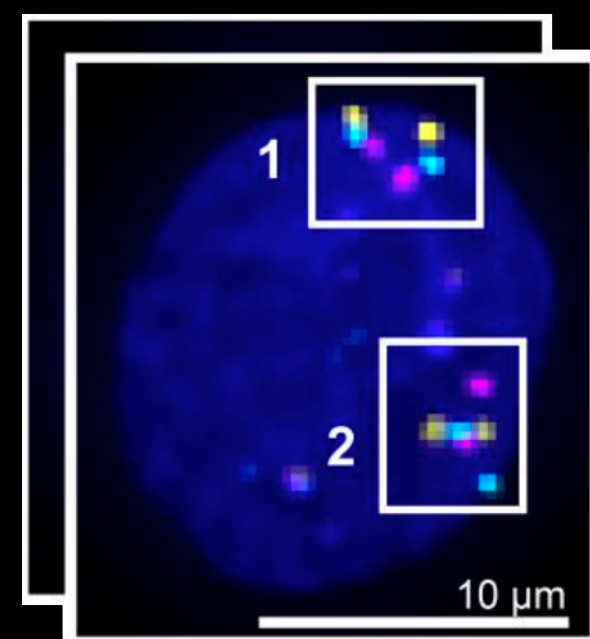
1

OligoSTROM
1 round
(2h/round)



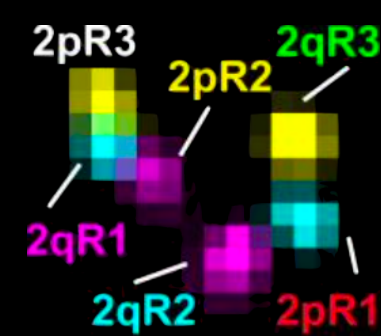
2

OligoFISSEQ
2 round
(3h/round)



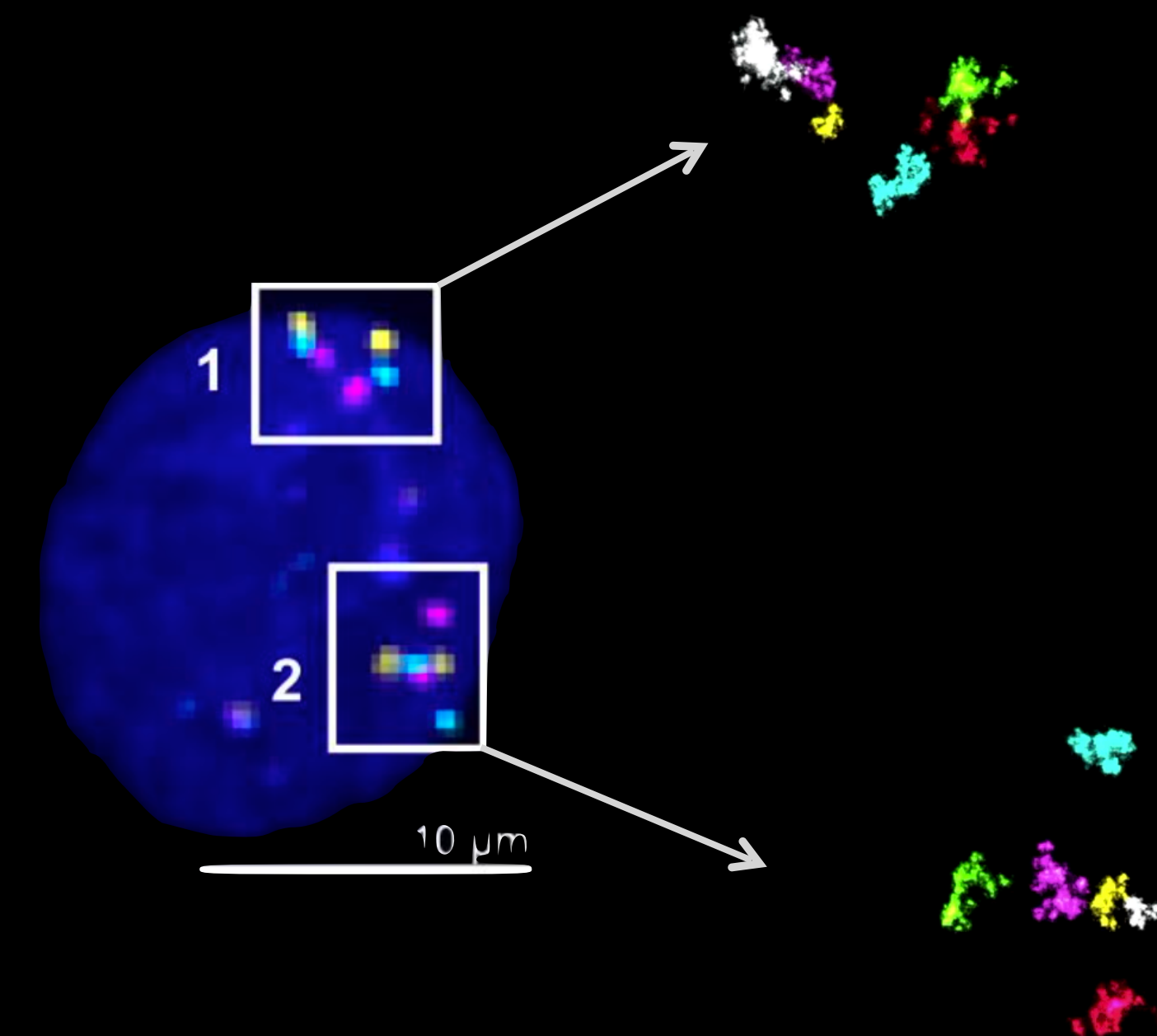
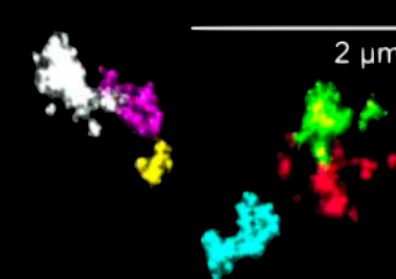
3

Decoding
OligoFISSEQ



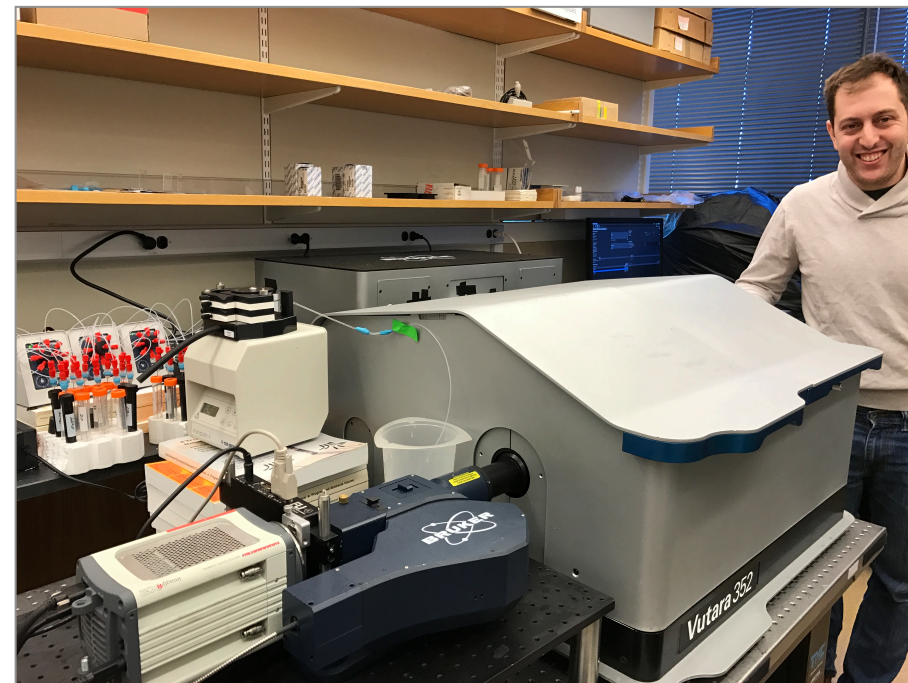
4

Mapping
OligoSTROM



High-resolution imaging

Tracing chromosomes with OligoSTORM & fluidics cycles in PGP1 cells



Guy Nir Harvard Med School

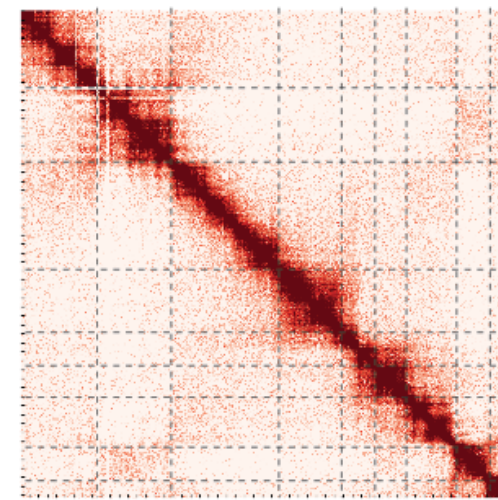
Bodgan Bintu Harvard

Carl Ebeling Bruker

Jeff Stuckey Bruker

John Schreiner Zero Epsilon

Steve Callahan Zero Epsilon



chr19:7,335,095-15,449,189
~8Mb



High-resolution imaging

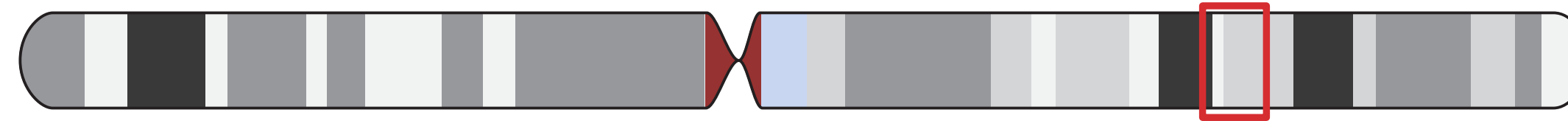
Tracing chr19:7,335,095-15,449,189 ~8Mb



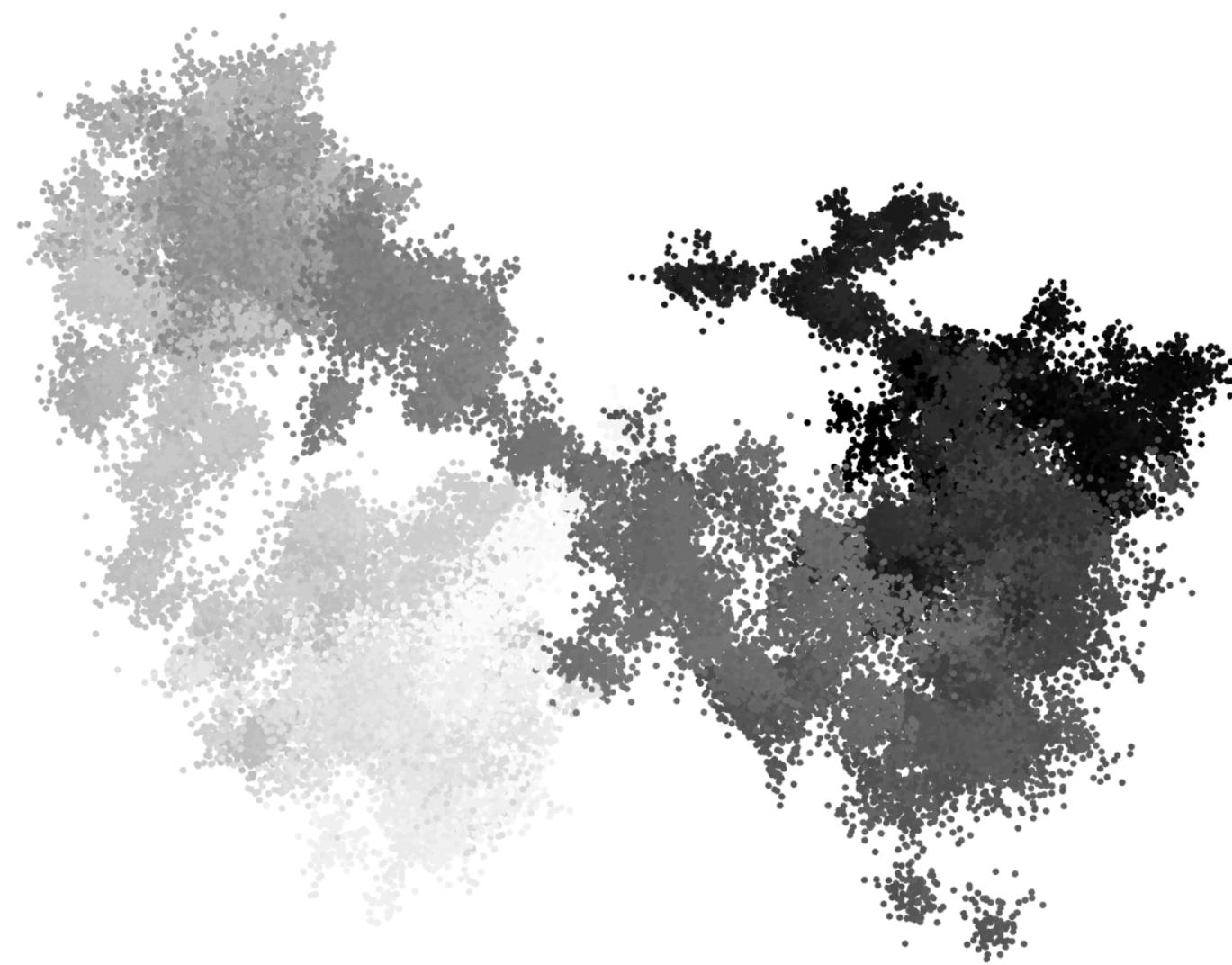
Integrating Hi-C and Imaging

SHAKER, integrating Hi-C and STORM

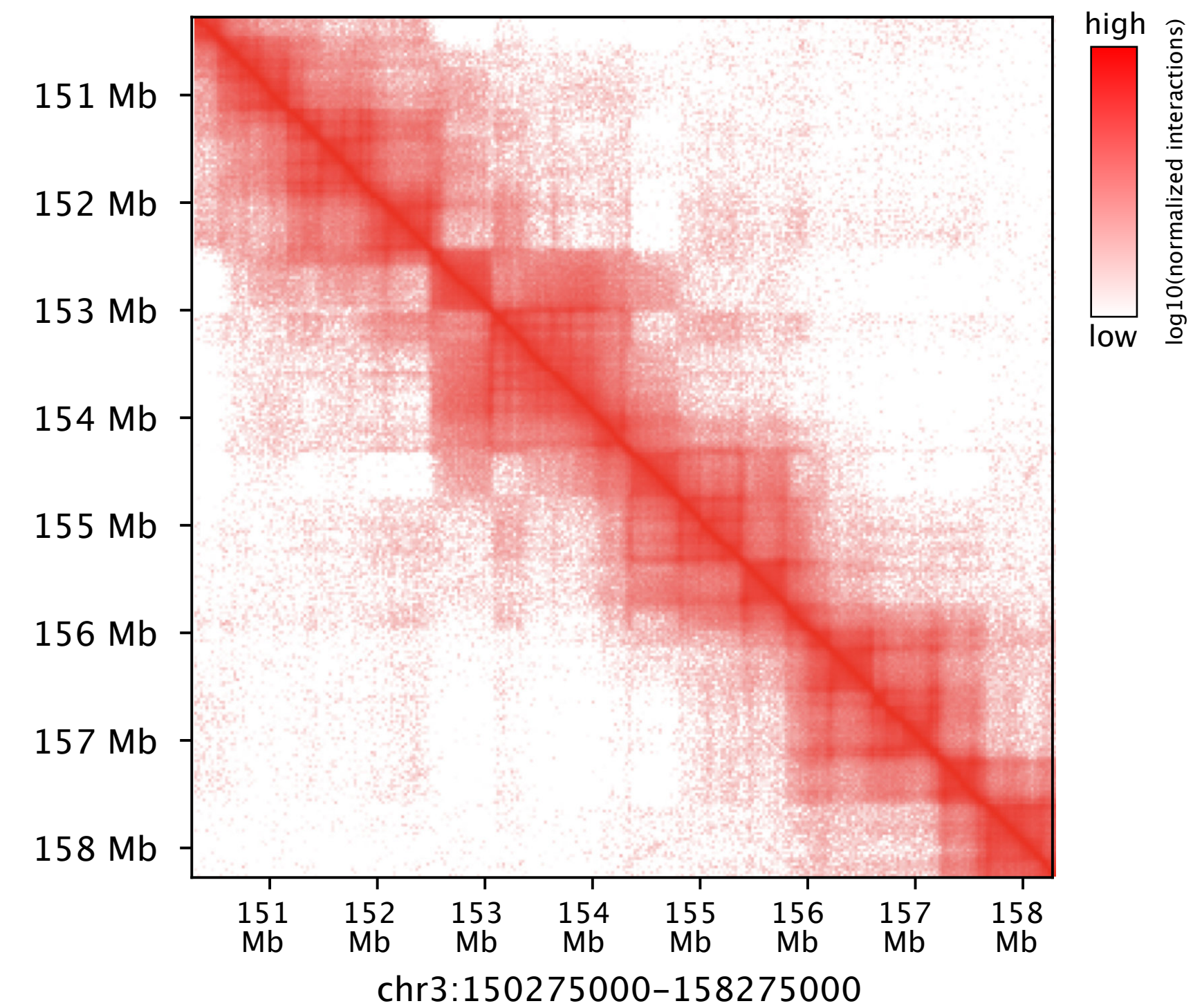
chr3:150,282,213-158,282,211



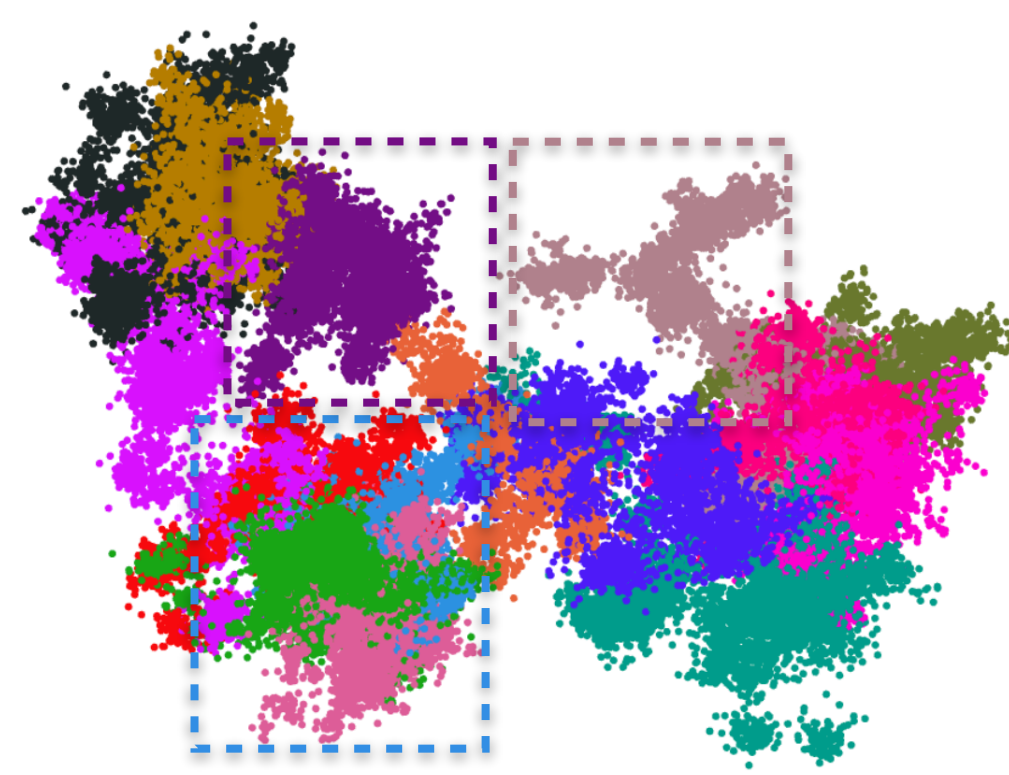
Hi-C genome-wide @1kb



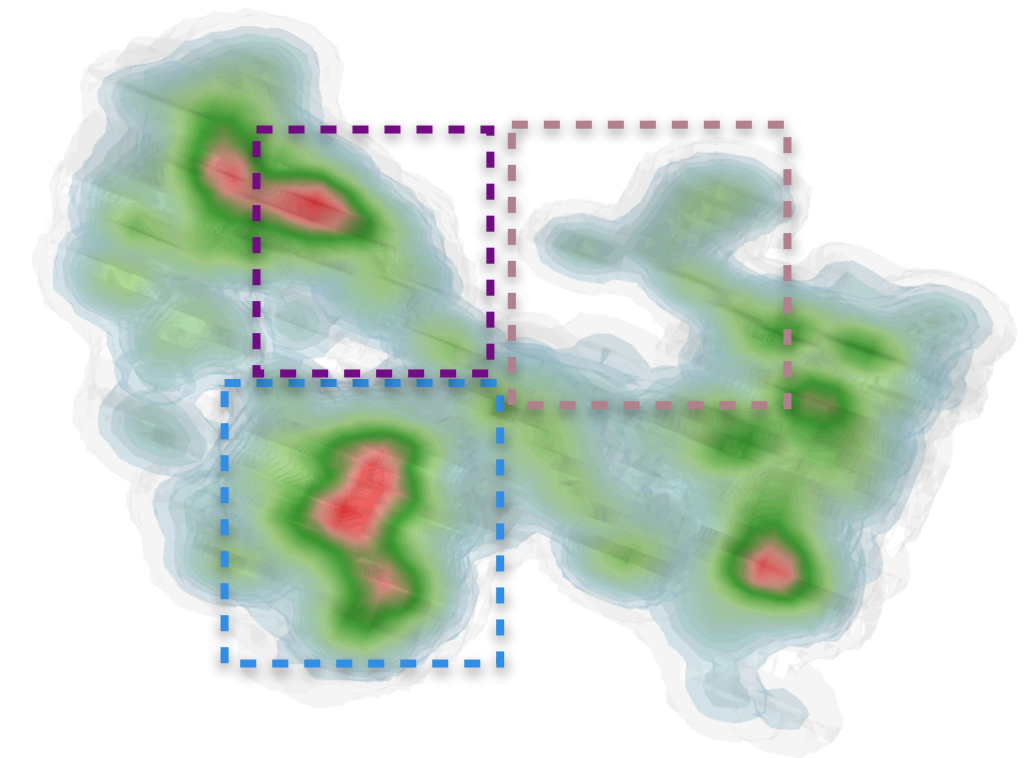
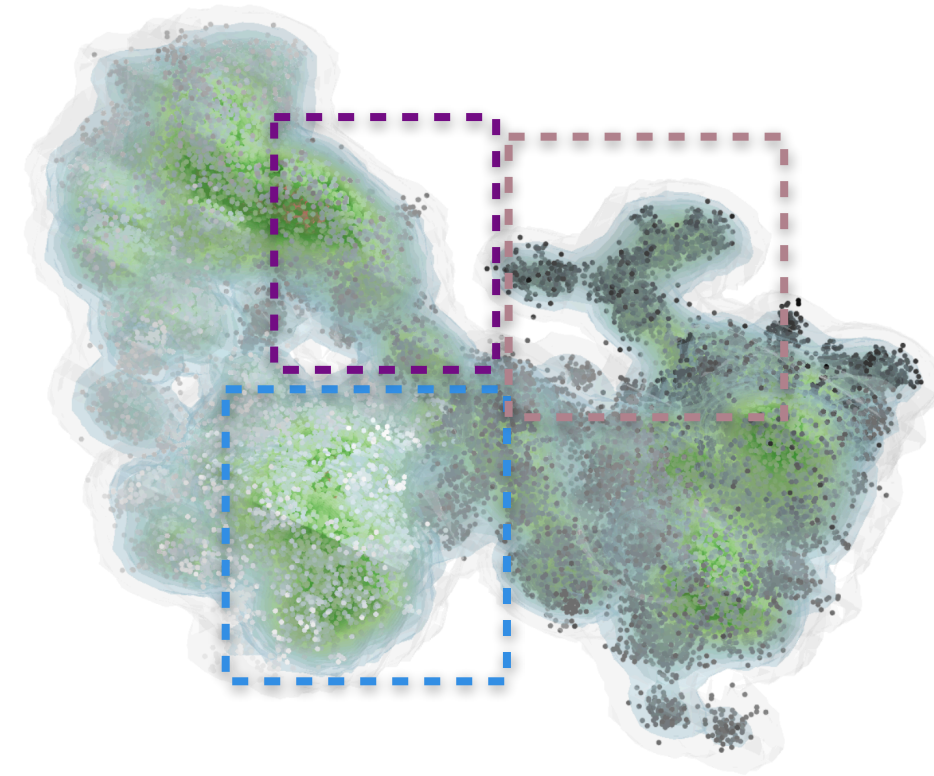
Hi-C map @25kb



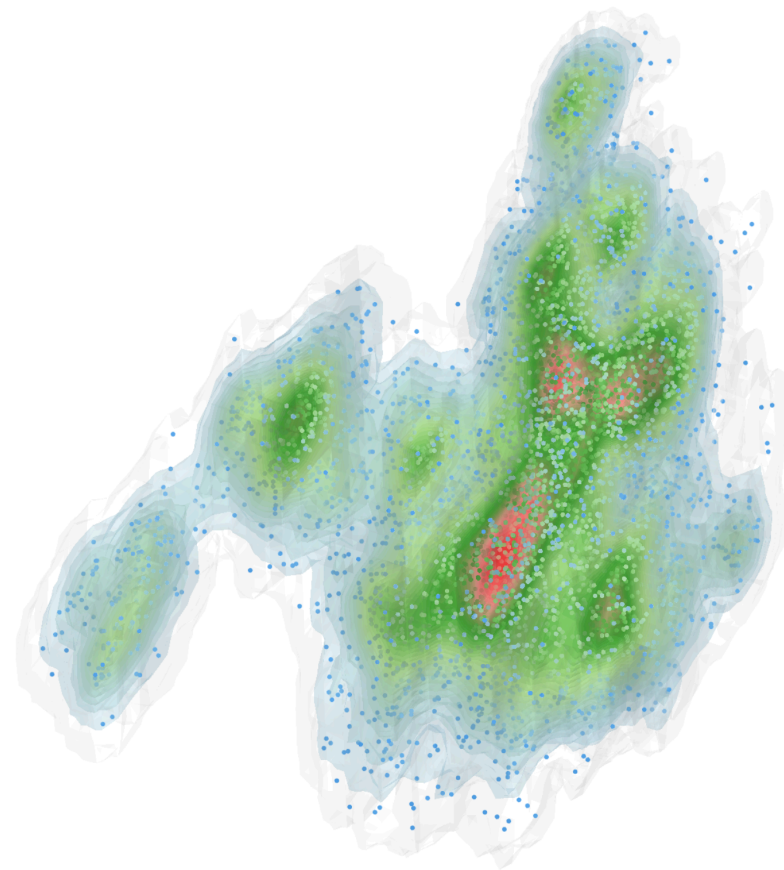
Imaging data processing



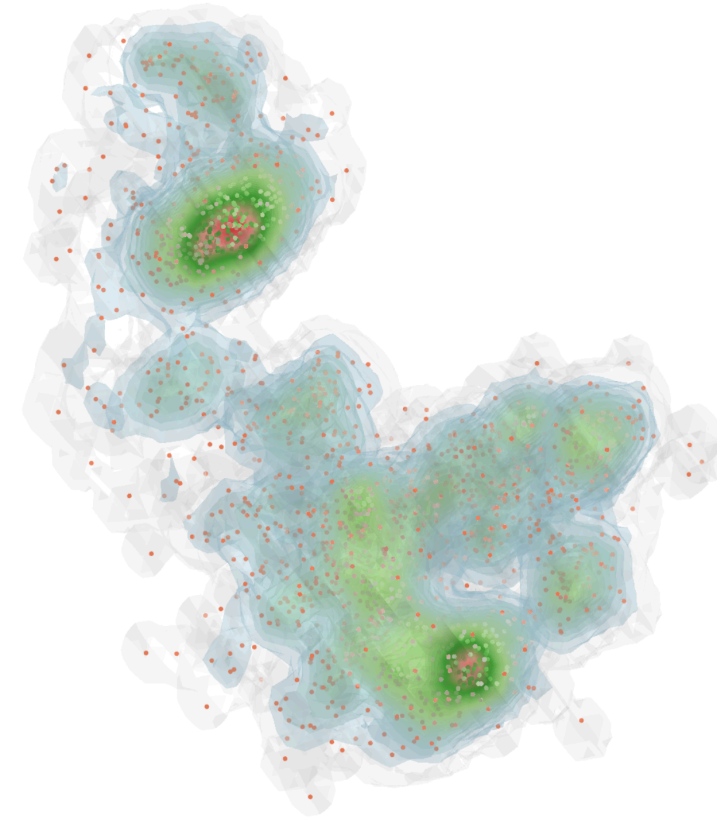
- Step 1
- Step 2
- Step 3
- Step 4
- Step 5
- Step 6
- Step 7
- Step 8
- Step 9
- Step 10
- Step 11
- Step 12
- Step 13
- Step 14
- Step 15



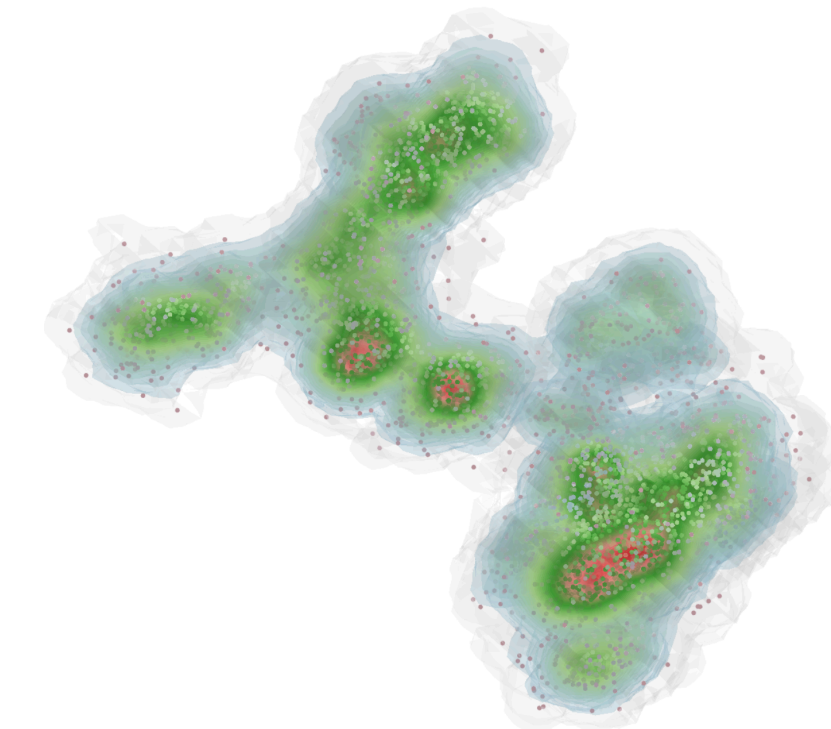
- dense  + dense



Step #1 chr3:150,282,213-150,782,213 (0.5Mb)

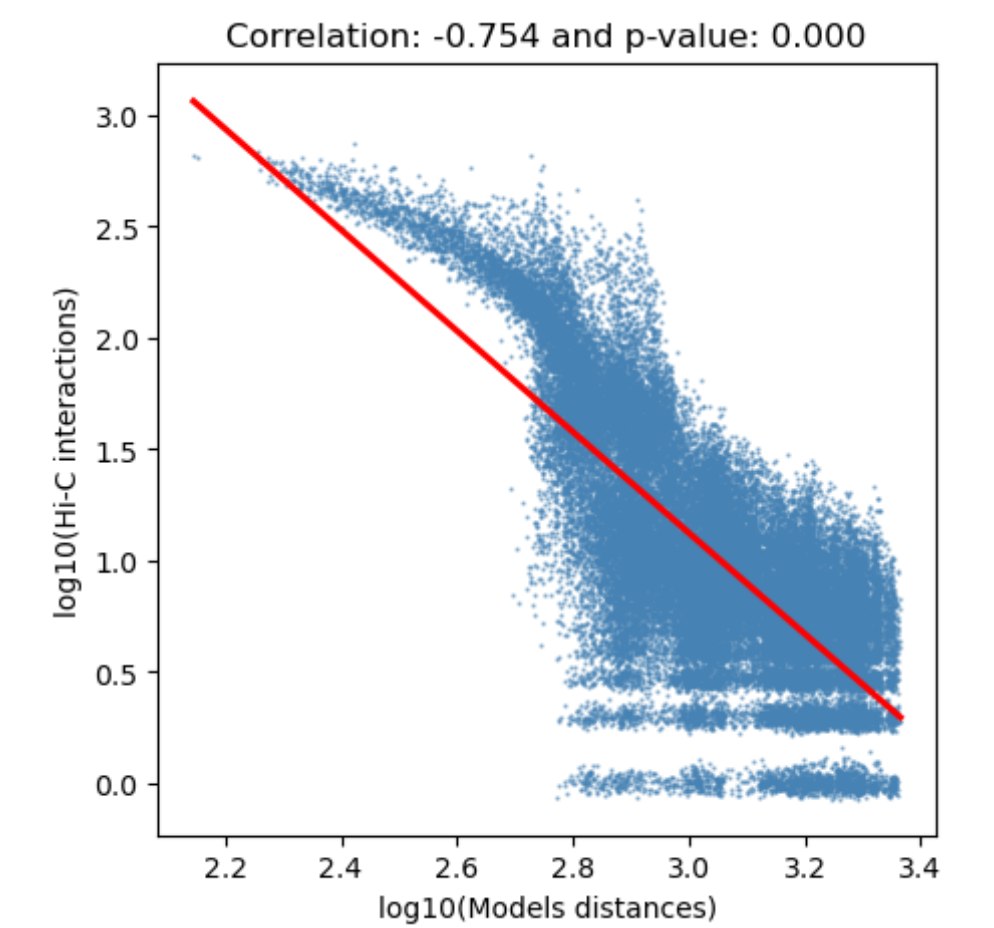
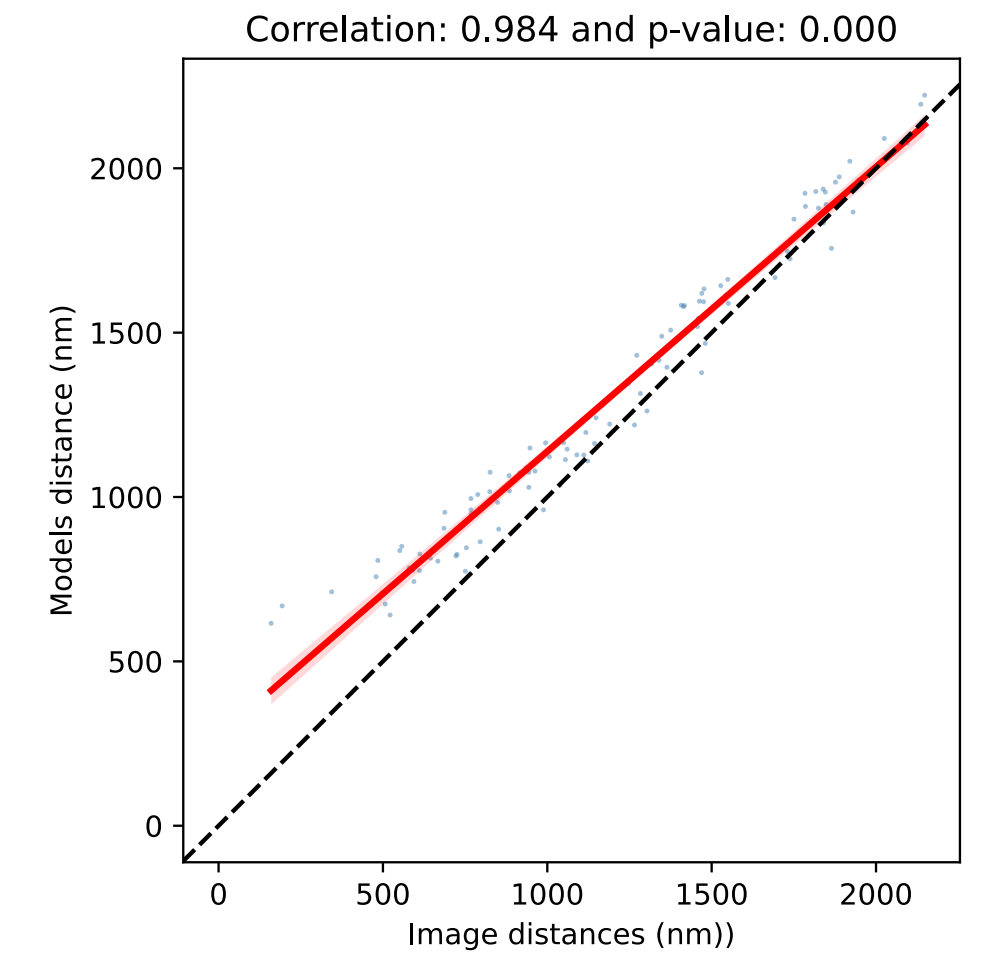
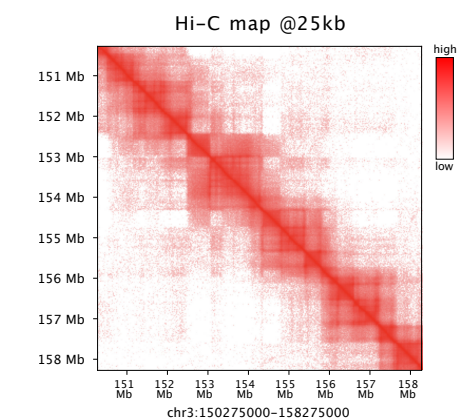
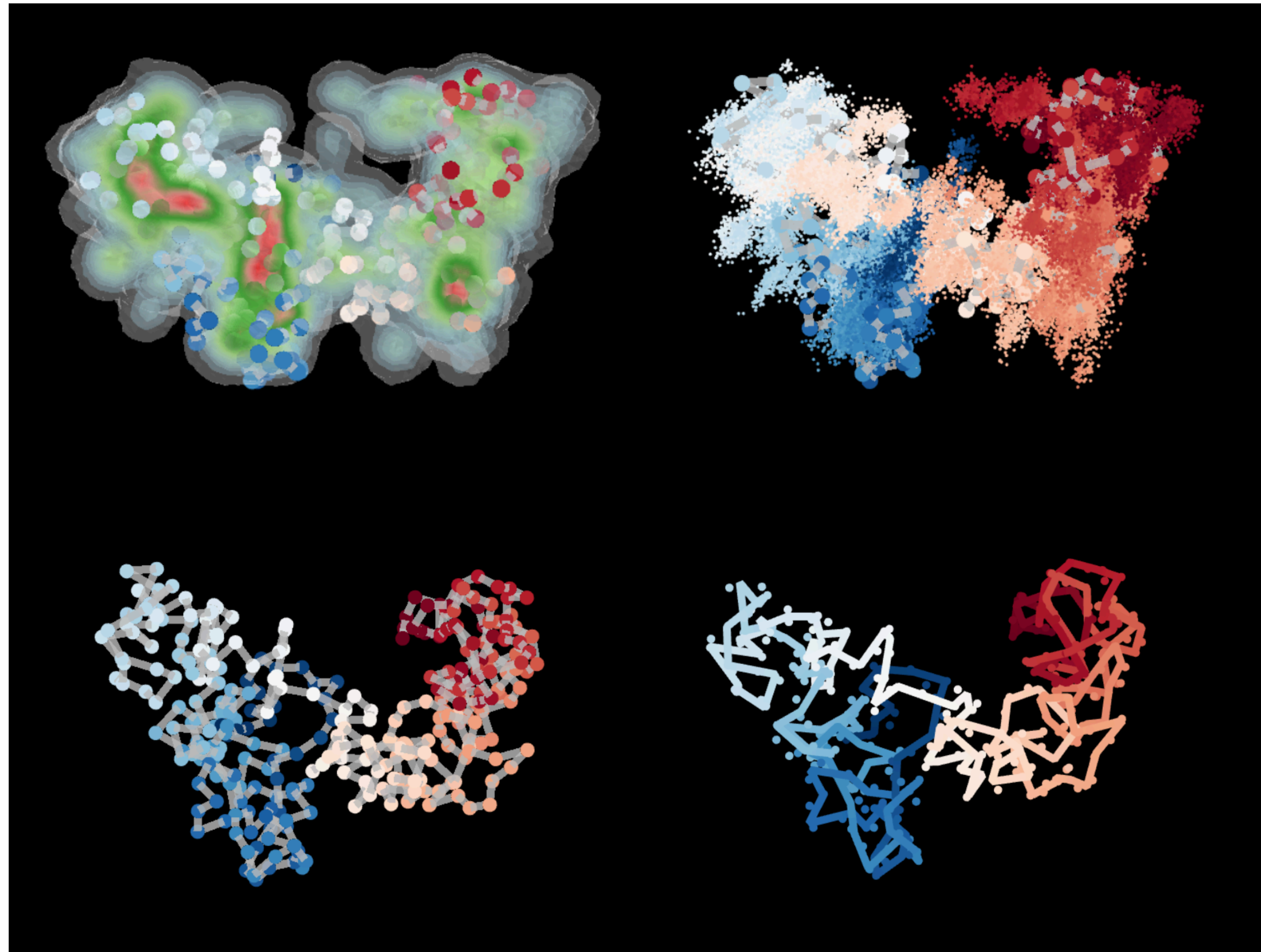


Step #8 chr3:154,782,211-155,282,211(0.5Mb)

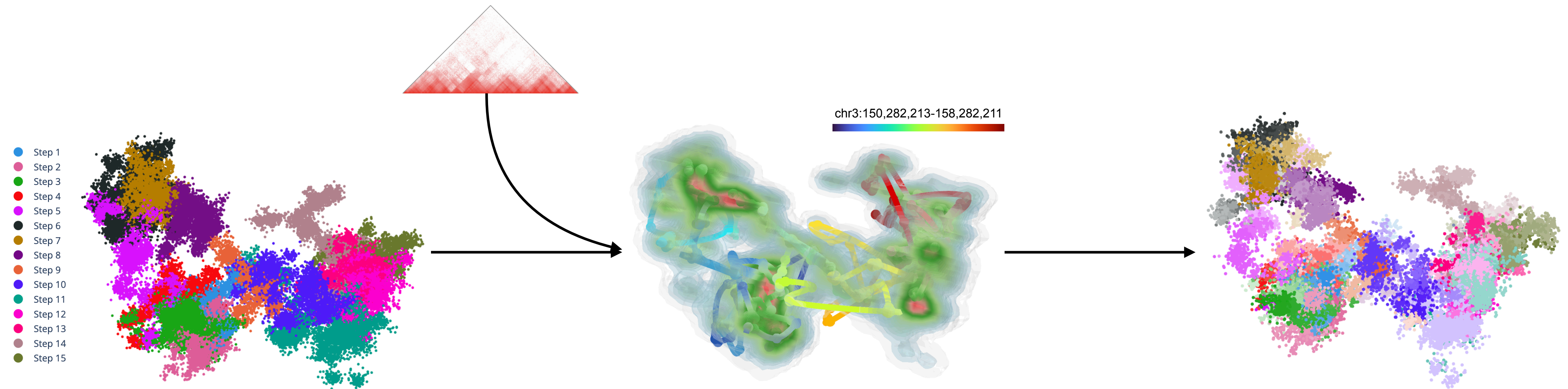
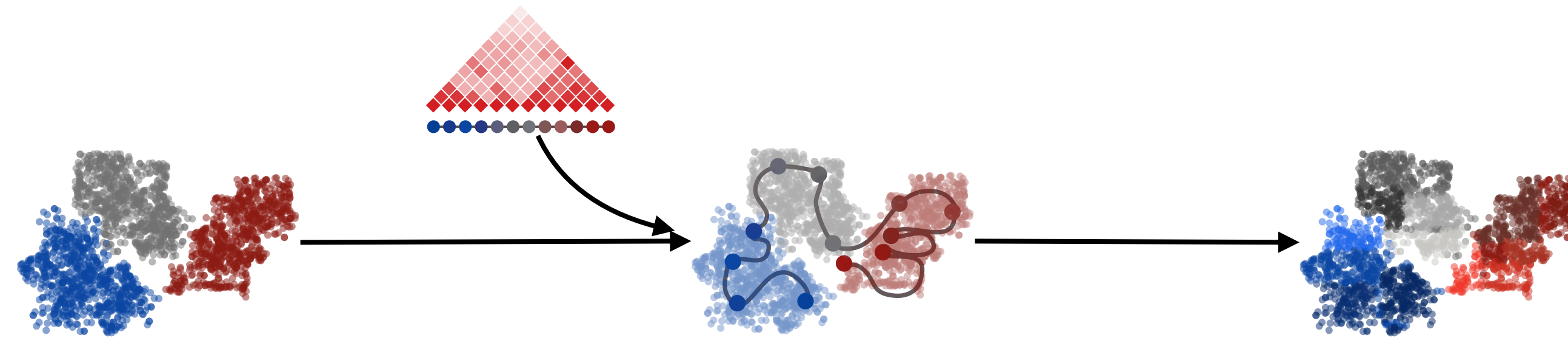


Step #14 chr3:156,782,211-157,282,211 (0.5Mb)

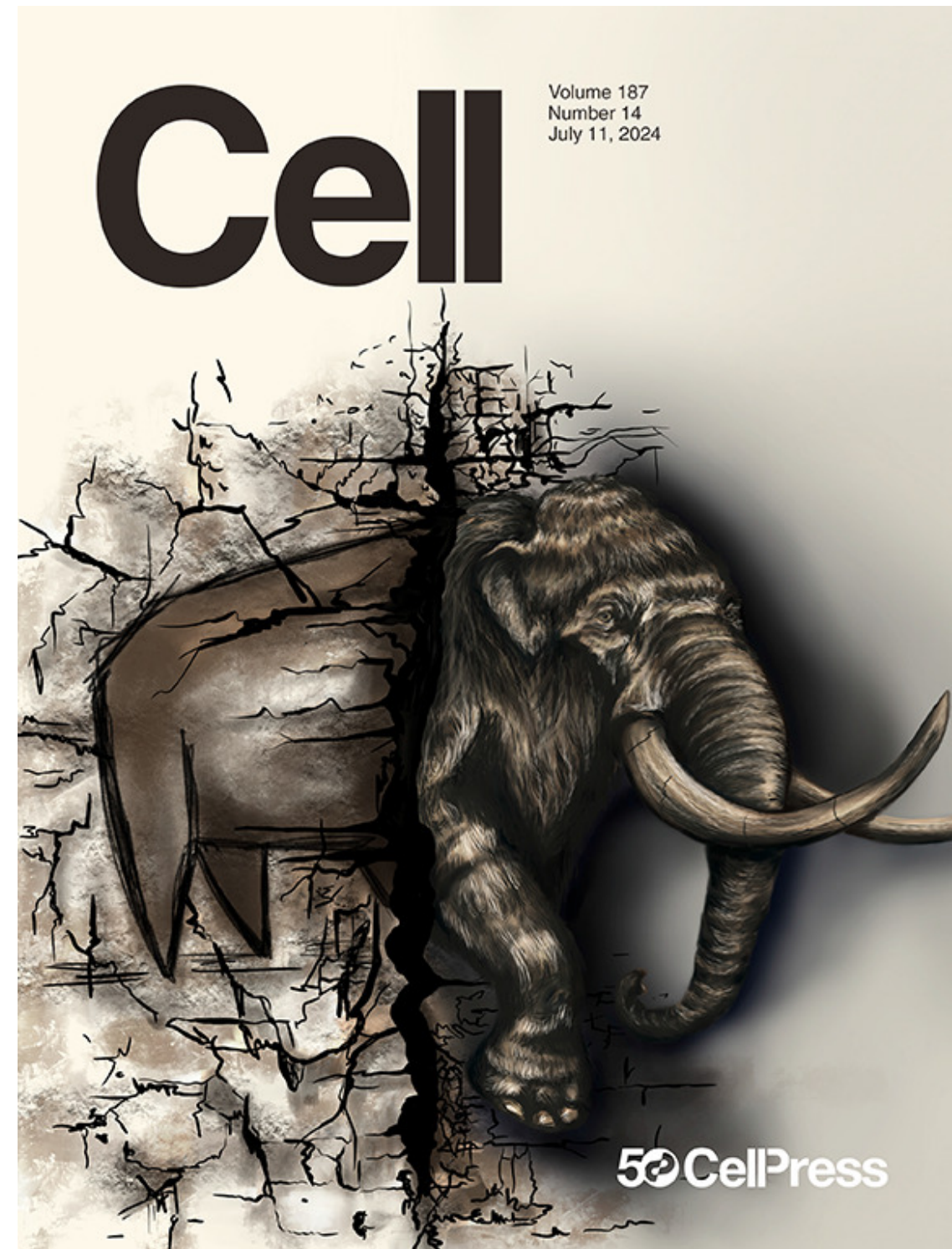
Full model of 8Mb in human chromosome 3



Effectively addressing the challenge of sequential STORM

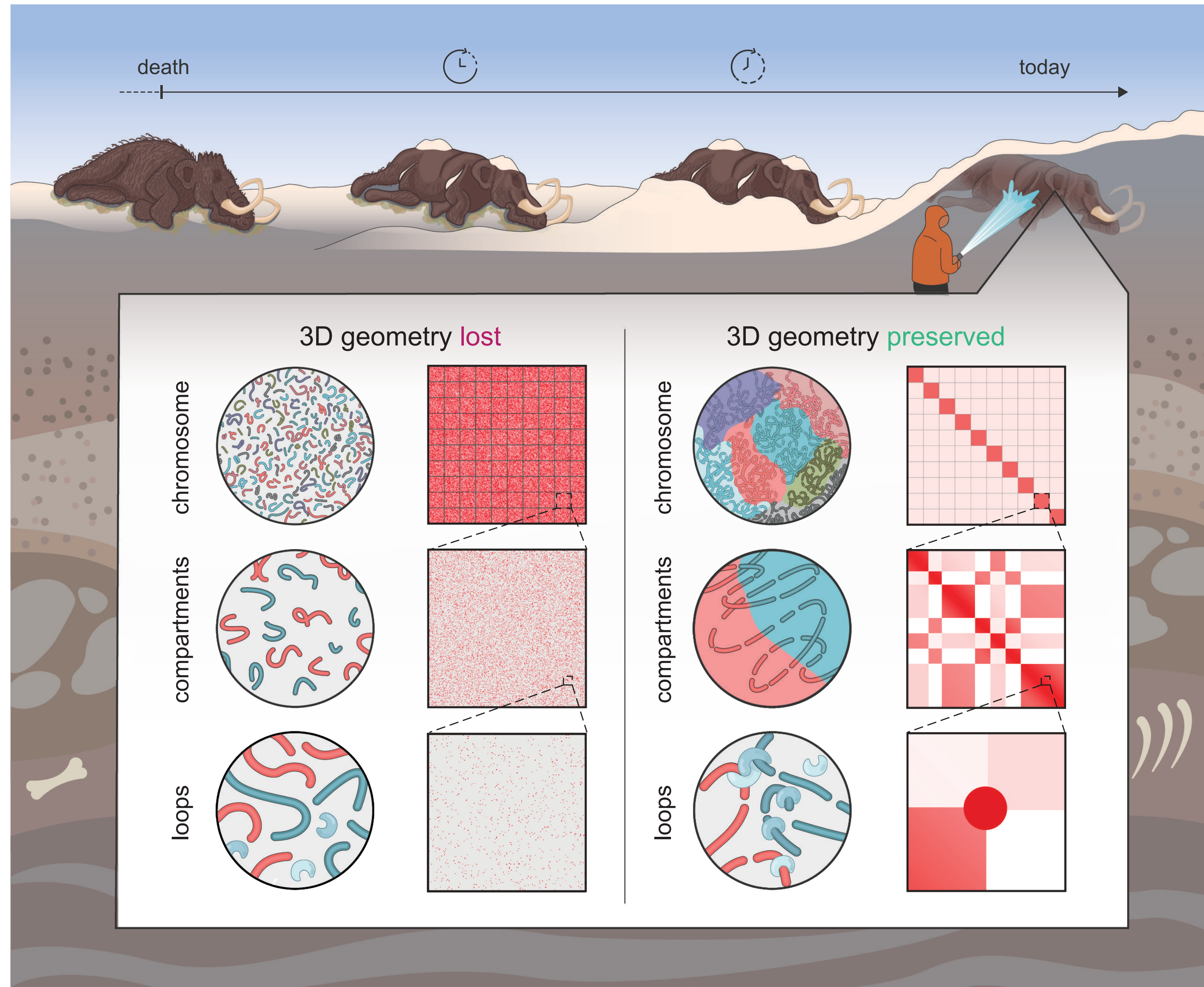


Other challenges.... “Difficult” samples



Cell (2024) 187 3541–3562

What happens to the nucleus in 52,000 years old?



A “woolly” phenomenal sample



Dan Fisher

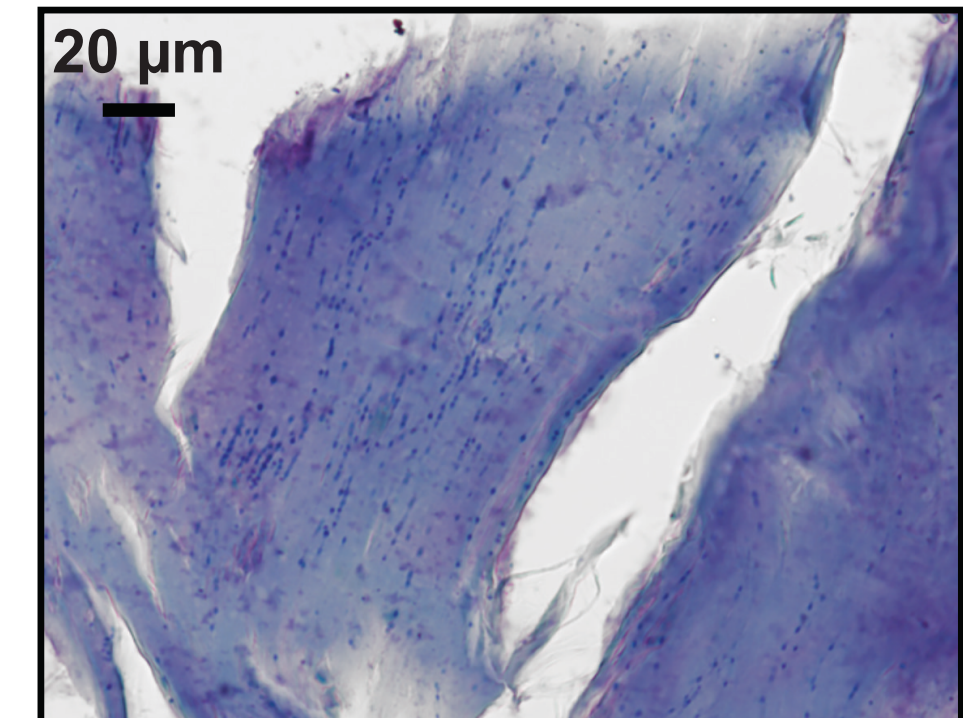
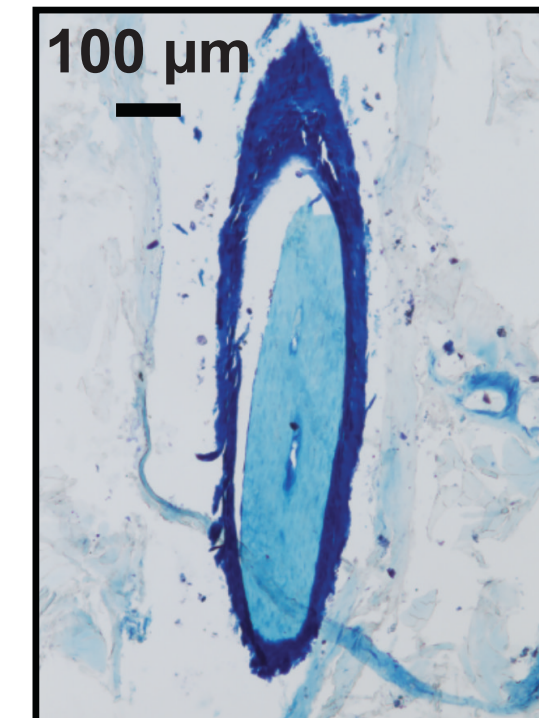
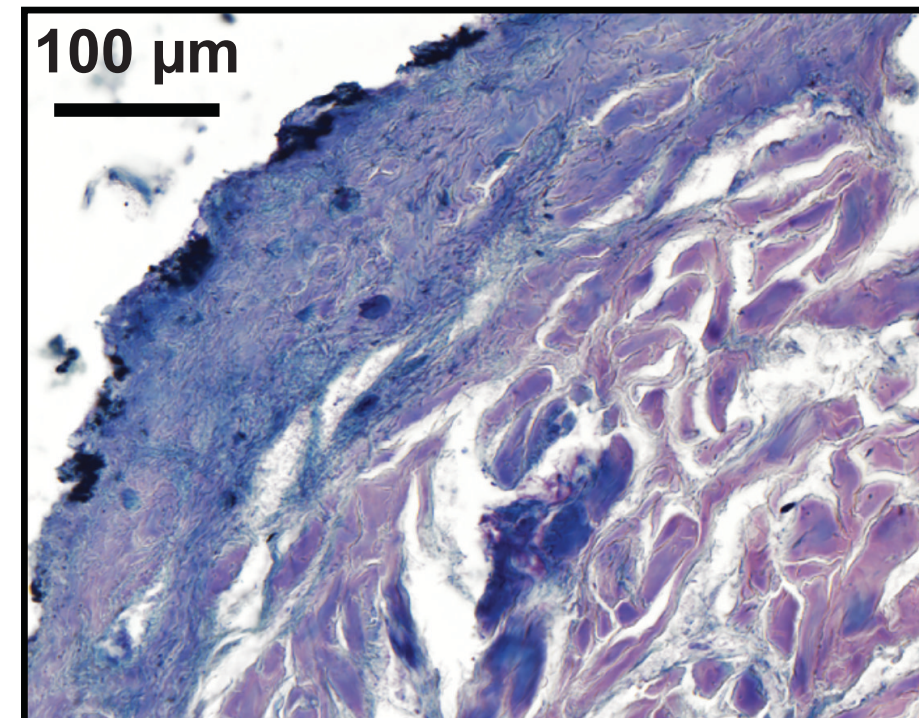
UMich, Museum of Paleontology

Valeri Plotnikov

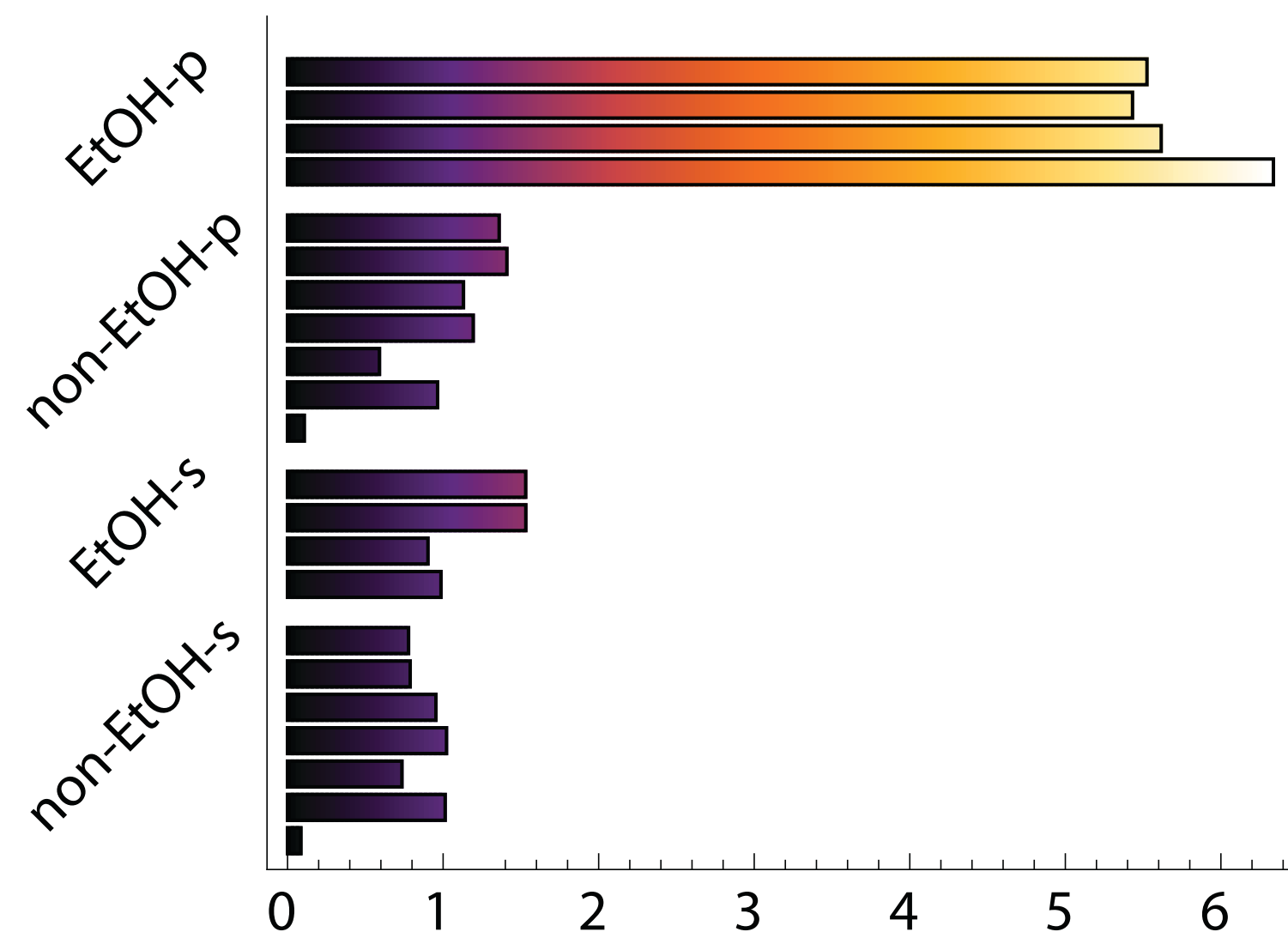
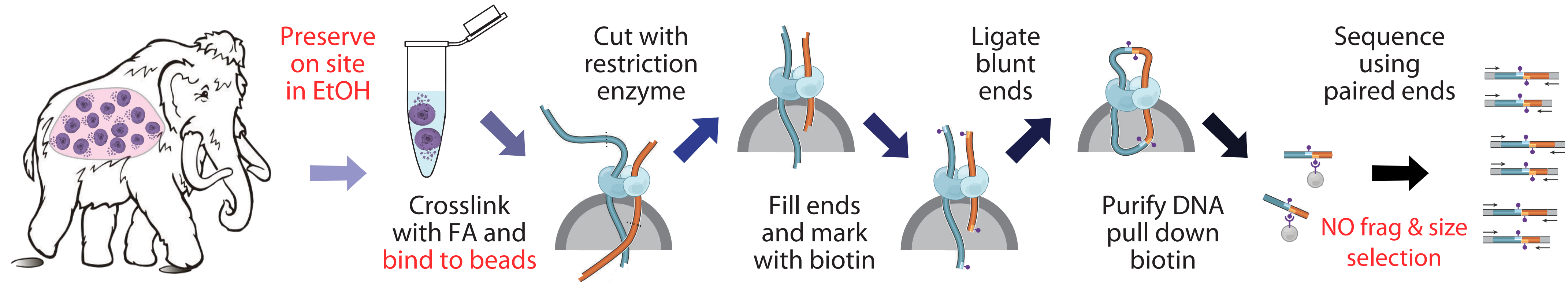
Sakha Academy of Sciences

- Found in permafrost in the summer of 2018
- Belaya Gora in Yakutia, Russia
- Date beyond the range of radiocarbon dating but older than >45,000 years

Photo credit: Chris Waddle

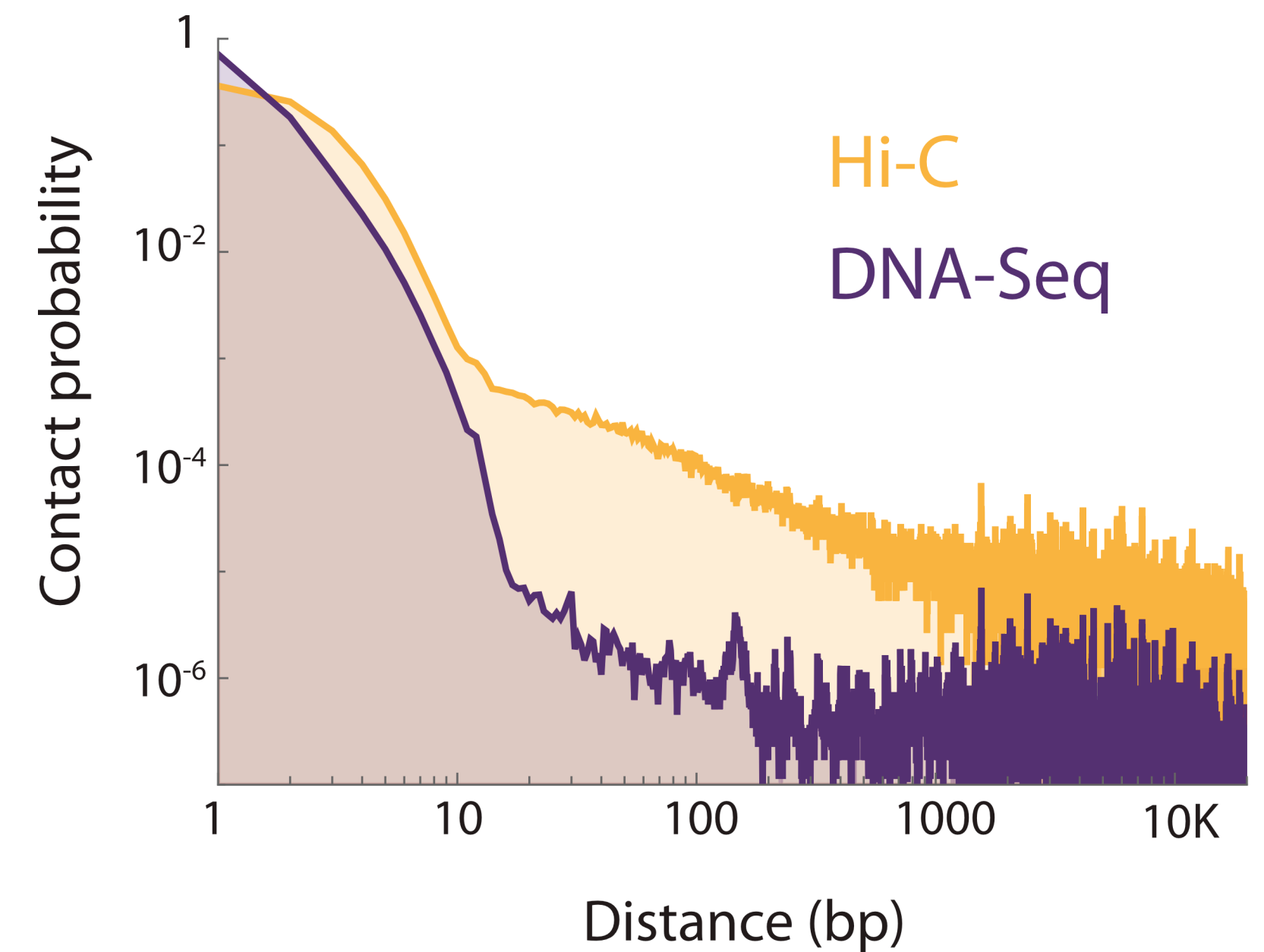


Paleo-HiC improves endogenous long-range contact recovery



% of Hi-C read pairs aligning to loxAfr3

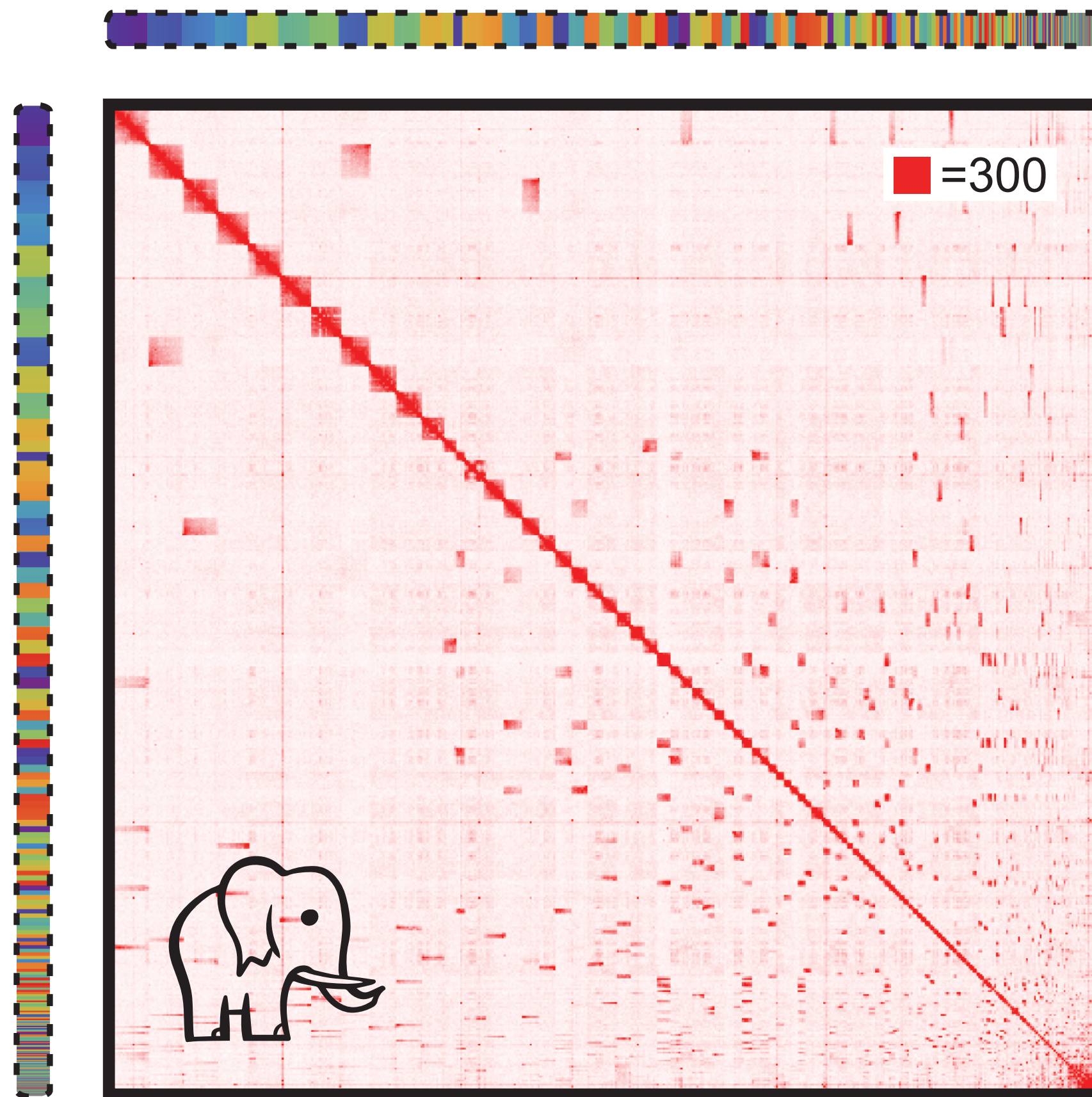
Total read count	4,444,894,354
Unique paired alignments (loxAfr3)	24,415,411
Unique paired (%)	0.55%
Long-range (20kb)	1,763,225
Long-range (%)	0.04%



This is a Hi-C from mammoth

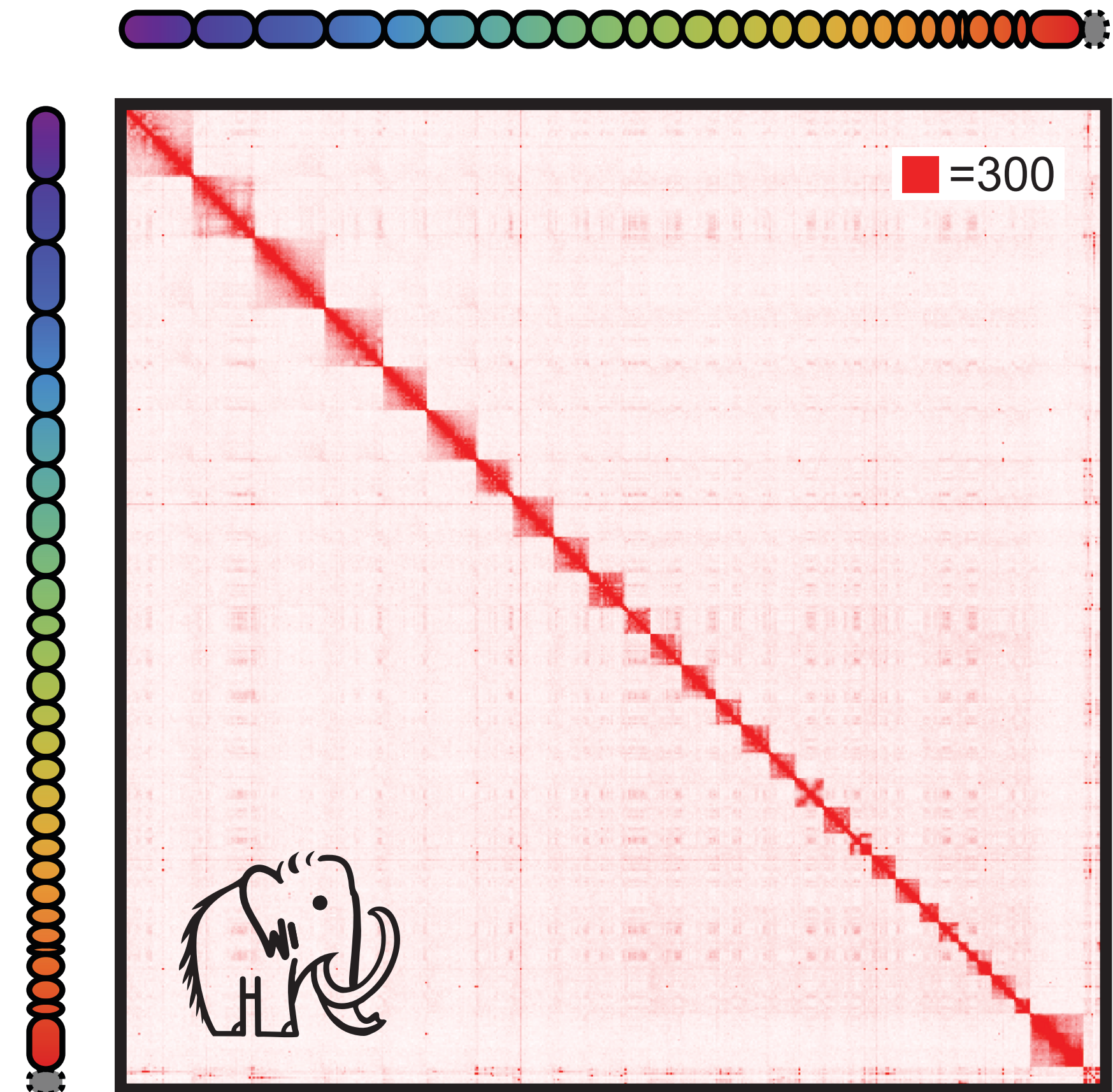
based on Loxafr3.0

PaleoHi-C vs Loxafr3.0,
fragmentary African elephant assembly

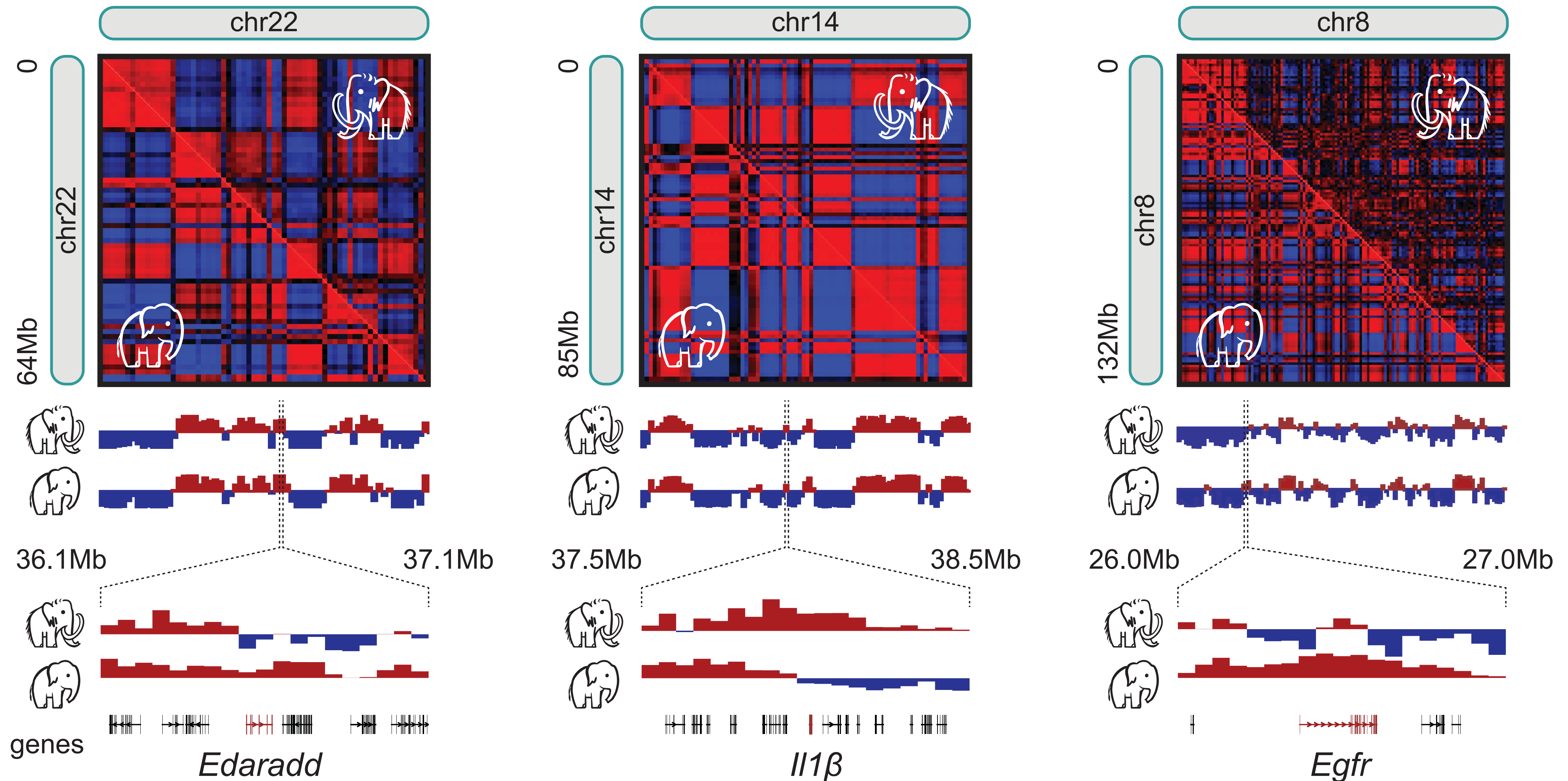


PaleoHi-C vs MamPri_Loxafr3.0_assisted_HiC,
chromosome-length mammoth assembly

3D assisted
assembly
→

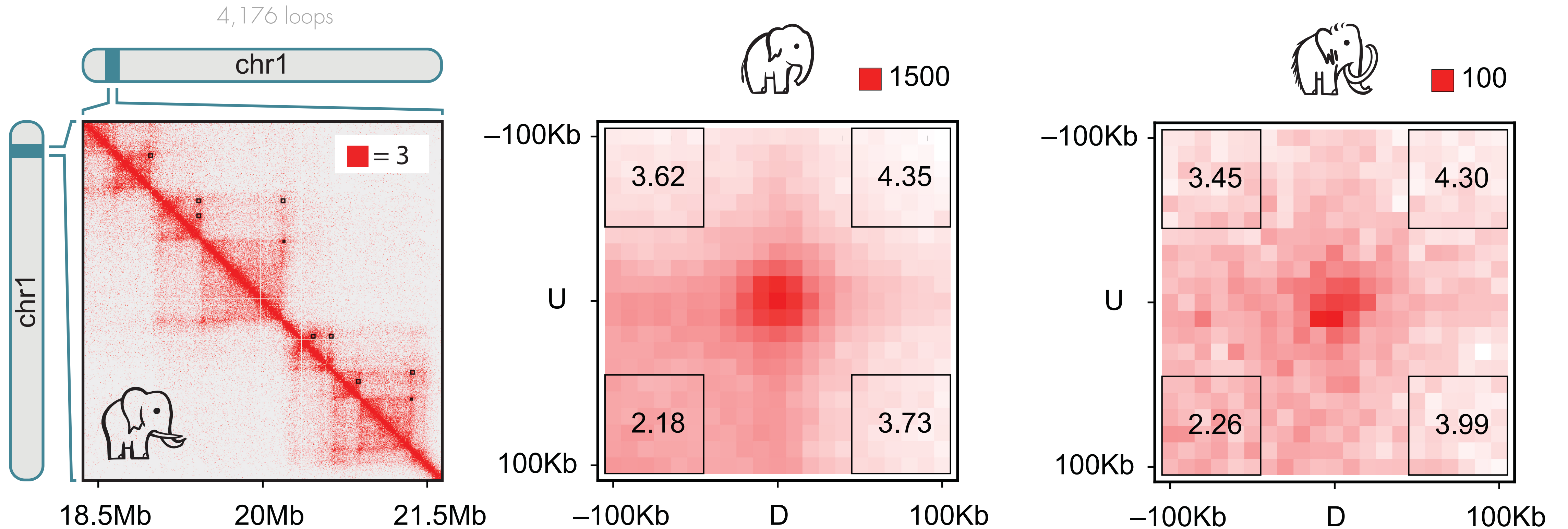


52 Mammoth Altered Regulation Sequences (MARS)



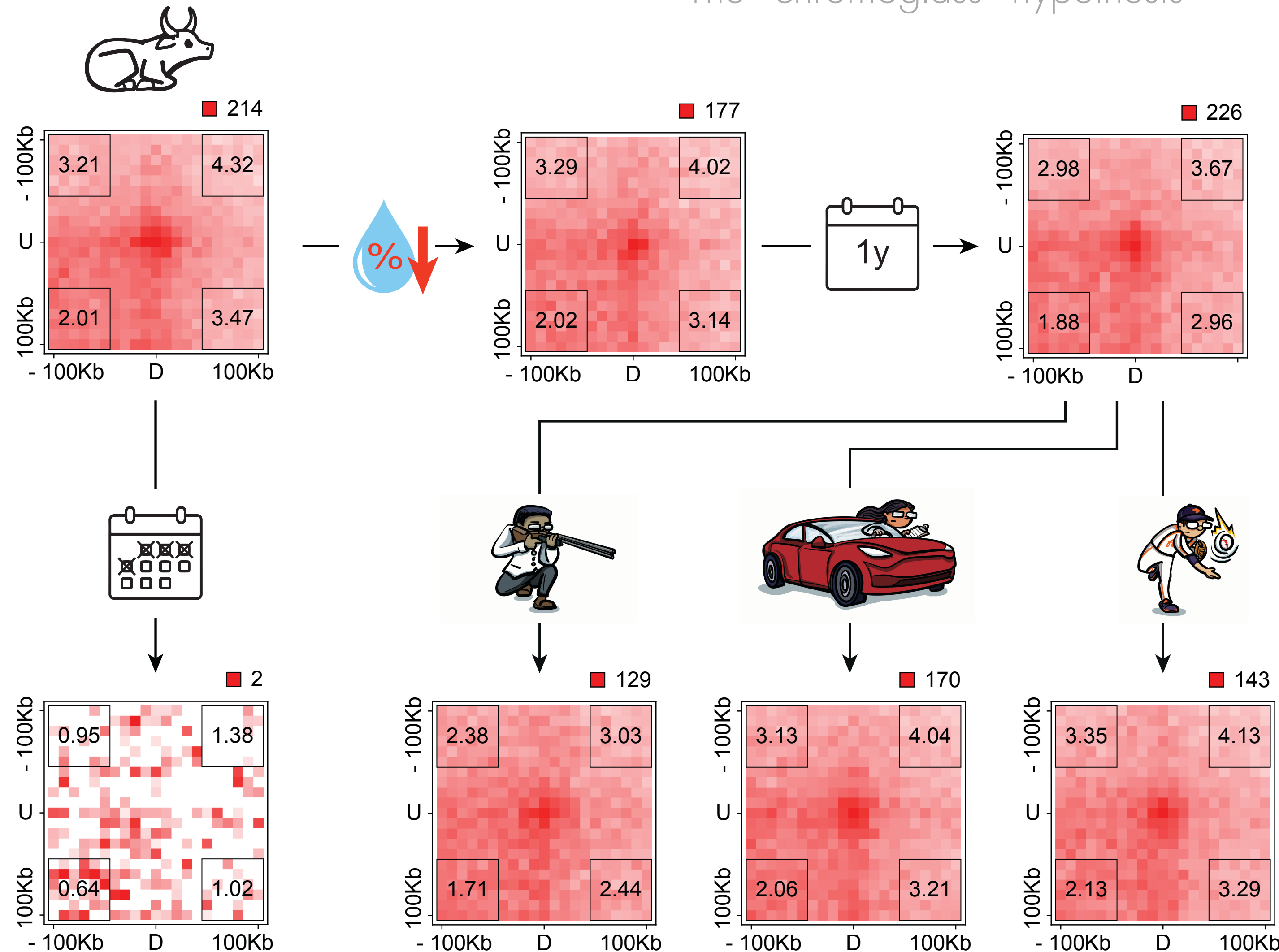
Paleo-hic recovers loop signatures!

Rao, Huntley et al., Cell 2014



How is this possible?

The "chromoglass" hypothesis



THREE-DIMENSIONAL GENOME ARCHITECTURE PERSISTS IN A 52,000-YEAR-OLD WOOLLY MAMMOTH SKIN SAMPLE

Marcela Sandoval-Velasco[#], Olga Dudchenko^{#,†}, Juan Antonio Rodríguez[#], Cynthia Pérez Estrada[#], Marianne Dehasque, Claudia Fontseré, Sarah S.T. Mak, Ruqayya Khan, Vinícius G. Contessoto, Antonio B. Oliveira Junior, Achyuth Kalluchi, Bernardo J. Zubillaga Herrera, Jiyun Jeong, Renata P. Roy, Ishawnia Christopher, David Weisz, Arina D. Omer, Sanjit S. Batra, Muhammad S. Shamim, Neva C. Durand, Brendan O’Connell, Alfred L. Roca, Maksim V. Plikus, Mariya A. Kusliy, Svetlana A. Romanenko, Natalya A. Lemskaya, Natalya A. Serdyukova, Svetlana A. Modina, Polina L. Perelman, Elena A. Kizilova, Sergei I. Baiborodin, Nikolai B. Rubtsov, Gur Machol, Krishna Rath, Ragini Mahajan, Parwinder Kaur, Andreas Gnirke, Isabel Garcia-Treviño, Rob Coke, Joseph P. Flanagan, Kelcie Pletch, Aurora Ruiz-Herrera, Valerii Plotnikov, Innokentiy S. Pavlov, Naryya I. Pavlova, Albert V. Protopopov, Michele Di Pierro, Alexander S. Graphodatsky, Eric S. Lander, M. Jordan Rowley, Peter G. Wolynes, José N. Onuchic, Love Dalén, Marc A. Marti-Renom[†], M. Thomas P. Gilbert[†], Erez Lieberman Aiden[†]

Cell 2024



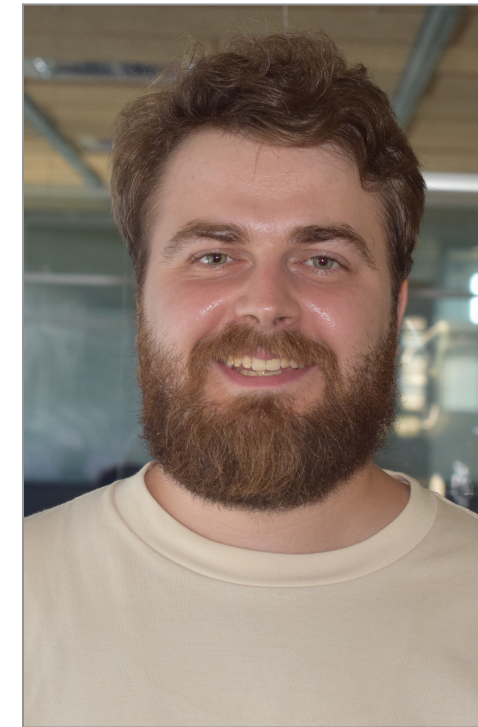
Discussion points (Tech)

1. What techniques are best?
2. How imaging can help?
3. What samples we need?

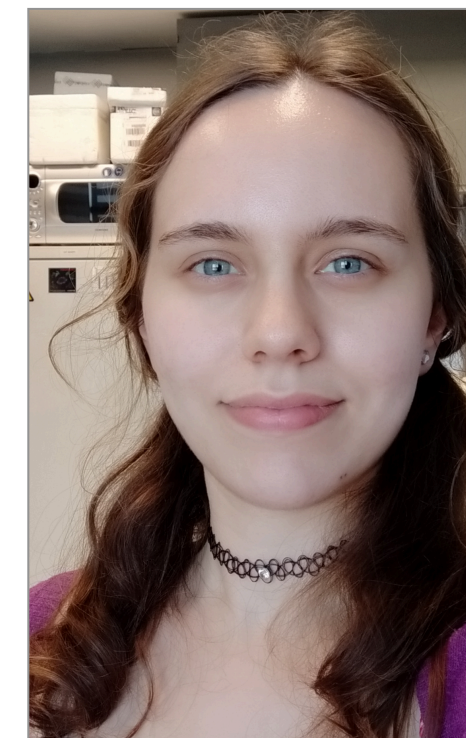
Discussion points (Concepts)

1. To TAD or not to TAD?
2. Loops, or else?
3. If it is dynamic, what do we care then?

Alexander Barclay
Nikolai Bykov
Iana Kim
Peter Hoboth
Anne Lee
Iago Maceda
John Markham



Maria Marti-Marimon
Ana Nikolovska
Mireia Novell
Merixell Novillo
Maria Roy
Aleksandra Sparavier
Leo Zuber



.: Our current sponsors :.

